Frontiers in Earth Science

TYPE Review
PUBLISHED 12 September 2022
DOI 10.3389/feart.2022.977250

OPEN ACCESS

EDITED BY
Luigi Jovane,
University of São Paulo, Brazil

REVIEWED BY
Firoz Badesab,
Council of Scientific and Industrial Research (CSIR), India
Juan Cruz Larrasoaña,
Instituto Geológico y Minero de España (IGME), Spain

*CORRESPONDENCE
Zhaoxia Jiang,
jiangzhaoxia@ouc.edu.cn

†These authors share first authorship

SPECIALTY SECTION
This article was submitted to Geomagnetism and Paleomagnetism, a section of the journal Frontiers in Earth Science

RECEIVED 24 June 2022
ACCEPTED 19 August 2022
PUBLISHED 12 September 2022

CITATION
Chen L, Guan Y, Zhou L, Yin Z and Jiang Z (2022), Variability of indian monsoon and its forcing mechanisms since late quaternary.
Front. Earth Sci. 10:977250.
doi: 10.3389/feart.2022.977250

Variability of indian monsoon and its forcing mechanisms since late quaternary

Liang Chen[1,2†], Yulong Guan[3†], Liang Zhou[3], Zhengxin Yin[1,2] and Zhaoxia Jiang[3,4*]

[1]South China Sea Marine Survey and Technology Center, State Oceanic Administration, Guangzhou, China, [2]Key Laboratory of Marine Environmental Survey Technology and Application, Ministry of Natural Resources, Guangzhou, China, [3]Frontiers Science Center for Deep Ocean Multispheres and Earth System, Key Lab of Submarine Geosciences and Prospecting Techniques, MOE, College of Marine Geosciences, Ocean University of China, Qingdao, China, [4]Laboratory for Marine Geology, and Laboratory for Marine Mineral Resources, Qingdao National Laboratory for Marine Science and Technology, Qingdao, China

The Indian monsoon is an important part of the global monsoon system, allowing important transfers of moisture at a large geographical scale and deeply affecting human populations and economic prosperity of regions. The tropical summer monsoon in the Northern Hemisphere is generally considered to be driven by low latitude solar radiation. Therefore, the summer monsoon strength is near zero-phase to the maximum of Northern Hemisphere Summer Insolation (NHSI). However, records from the Arabian Sea and some other parts of the Indian Ocean (e.g., Andaman Sea) show that a ~8 kyr phase difference exists between the Indian summer monsoon (ISM) strength and the northern Hemisphere Summer Insolation maxima, which is obviously different from the records of stalagmites in the East Asia and other marine sediments (e.g., Bay of Bengal). This leads to the “sea-land precession phase paradox” in indian summer monsoon research. This paper systematically summarizes the Indian monsoon variability on orbital scale indicated by various records from the Indian monsoon regions (including oceans and continents) since the late Quaternary. The orbital forcing of Indian monsoon, the potential phase difference between indian summer monsoon and northern Hemisphere Summer Insolation and its possible forcing mechanism(s) are further discussed. The observed phase lag between indian summer monsoon and northern Hemisphere Summer Insolation may be controlled by the Atlantic Meridional Overturning Circulation (AMOC), latent heat transfer between the southern Indian Ocean and the Asian continent, or caused by the lack of tightly coupling between the Arabian Sea summer monsoon proxies and the monsoon intensity. In addition, it is still unclear whether previous monsoon proxies can provide a strong constraint on the intensity of summer monsoon. Environmental magnetism has been widely used in high-resolution dating and the analysis of paleoclimate variabilities in marine and terrestrial sediments, due to its high sensitivity on the rainfall and temperature. Therefore, in order to solve these issues, it is necessary to combine magnetic parameters with geochemical and paleontological parameters for more systematic work in the future.

KEYWORDS

indian monsoon, northern hemisphere summer insolation (NHSI), phase differences, indian ocean, environmental magnetism

1 Introduction

The Indian monsoon, or South Asian monsoon (Gupta and Anderson, 2005), a subsystem of the Asian monsoon, is an important part of the global monsoon system, and represents one of the Earth's most dynamic interactions between atmosphere, oceans and continents (Clemens et al., 1991). In boreal summer, the Indian summer monsoon (ISM), driven by the cross-equatorial pressure gradient between the Tibet Low in the Asian continent and the Mascrene High in the southern Indian Ocean (Webster et al., 1998; Boos and Kuang, 2010), controls the environment of Northern Indian Ocean and the seasonal climate of India, Myanmar, Indochina Peninsula and even Southwest China. In boreal winter, the reversal pressure gradient leads to the Northeast monsoon (Figure 1). The wet summer monsoon brings the dominant precipitation and potential geological disasters in the monsoon areas, which affects the human populations and economic prosperity of regions (Sinha et al., 2005; Hao et al., 2016; Wang et al., 2018; Cheng et al., 2020). Moreover, as two important subsystems of the Asian monsoon system, the Indian monsoon and the East Asian monsoon are both controlled by the seasonal land-sea thermal contrast. At the same time, the uplifting of the Tibetan Plateau, the ice sheet variabilities and the thermohaline circulation also affect the formations and evolutions of those two monsoons (e.g., Prell and Kutzbach, 1992; Rea, 1992; An

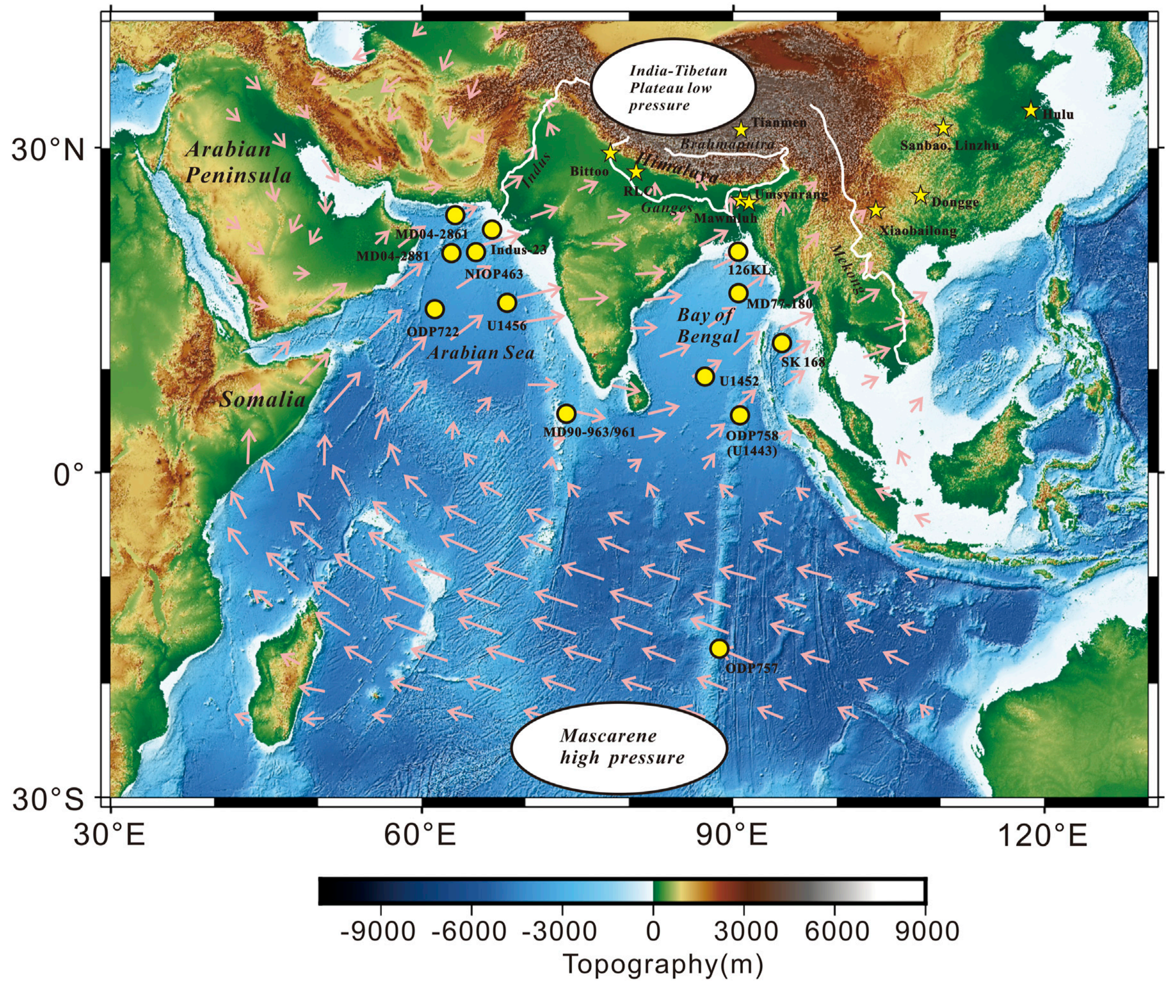

FIGURE 1
Location map showing marine sediment sites (yellow dots), terrestrial caves (yellow stars), and wind directions of the ISM (pink arrows).

et al., 2001, 2015; Clift et al., 2008; Wang, 2009; Deeken et al., 2011; Chen et al., 2014; Li et al., 2014; Betzler et al., 2016, 2018; Hao et al., 2016; Tada et al., 2016).

In the modern monsoon climatology, due to the increase of solar radiation in Northern Hemisphere, the thermal contrast between the Asian continent and the Indian-Pacific Ocean brings moisture-laden winds blowing from southwest-southeast to the continent during June-August as the Intertropical Convergence Zone (ITCZ) move northward. So, the strength of Northern Hemisphere summer monsoon corresponds to the maxima of Northern Hemisphere Summer Insolation (NHSI) (Kutzbach, 1981; Ruddiman, 2006; Wang, 2006, 2009; Wang et al., 2018; Cheng et al., 2019, 2021). The variation of solar radiation at the low latitude is the main driving force of the orbital-scale changes of summer monsoon (Kutzbach, 1981, 2008), therefore, precession is the main controlling factor of low latitude climate processes by regulating when the Earth reaches perihelion (Ruddiman, 2001; Wang et al., 2018).

Oxygen isotope records of stalagmites in East Asia indicate that the East Asian summer monsoon (EASM) has been dominated by the ~23 kyr precession cycles since the late Pleistocene, which is consistent with the traditional monsoon hypothesis that low latitude insolation forcing is dominant. However, a phase lag (~3 kyr) exists between the strength of EASM and the maxima of NHSI (e.g., Wang et al., 2001, 2008; Yuan et al., 2004; Ruddiman, 2006; Cheng et al., 2012, 2016), which is also observed between the East African monsoon strength and the maxima of NHSI reconstructed by Mediterranean sapropels (Lourens, 2004; Revel et al., 2010; Caley et al., 2011a). Marine sedimentary records from the Arabian Sea in the northern Indian Ocean, indicate that a phase lag of ~8 kyr exists between the marine primary productivity and the NHSI in precession-band (Clemens et al., 1991, 2008, 2010; Reichart et al., 1998; Clemens and Prell, 2003, 2007; Wang et al., 2005). Then, the question is the main forcing mechanism of this phase lag and whether it is a regional event or a common event.

The solutions to those problems are significant for understanding the evolution of Indian monsoon on the orbital-scale since the late Pleistocene. Therefore, in this paper, we aim to sort out the achievements and debates in the research of the variation and main driving factors of the Indian monsoon since the late Pleistocene, clarify the advantages of environmental magnetism on solving these problems, and puts forward prospects for future studies.

2 Proxies and paleo-monsoon variability

2.1 Monsoon proxies

Systematic studies on the Indian monsoon evolution since Pleistocene benefited from the long-term record of marine sediment, where the Arabian Sea coastal upwelling and the sapropel deposits from the Mediterranean are classic and most representative (Rossignol-Strick, 1983; Prell et al., 1984). These two records reflect the application of wind-based and rain-based proxies for the Indian and African monsoon, respectively. Generally, monsoon proxies can be classified into two categories depending on the primary aspects of the monsoon. One type is the proxies related to the winds (direction, strength and persistence), and the other is those associated with rainfall (Table 1) (Wang et al., 2005, 2014). In the Indian monsoon regions, upwelling is most frequently used to indicate the wind intensity (Clemens and Prell, 1991; Clemens et al., 1996; Ziegler et al., 2010a; Saraswat et al., 2019). The high abundance of microfossils (*G. bulloides* % and *G. ruber* %) in marine sediments at low latitudes is a major indicator of upwelling driven by the ISM (Kroon and Ganssen, 1989; Kroon et al., 1991; Jian et al., 2001). However, the microfossils are also sensitive to external environmental factors unrelated to the monsoon (Wang et al., 2014). Clemens et al. (1996) reconstructed the variability of ISM using the grain size of sediment ODP Site 722, and proposed that it could reflect the transport capacity of southwest monsoon. However, grain size is usually affected by some complex hydrodynamic conditions during sediment transport and accumulation, and cannot reflect the intensity of southwest monsoon simply. Therefore, Clemens and Prell (2003) took a multi-proxy approach to calculate the ISM factor by analyzing five proxies (grain size, Ba counts, $\delta^{15}N$, *G. bulloides*% and opal mass accumulation rate). However, limitations still exist because most of the five proxies are indicators of marine productivity. The high productivity may not only be induced by ISM, but also other process, such as changes in ocean nutrients related to ice-volume cycles and migration from the continental shelf (Ruddiman, 2006; Wang et al., 2014). Subsequently, the sequence of ISM variability was obtained by summing up numerous independent records of wind-driven productivity, including Ba counts, Ba/Al, Ti/Al, and planktonic foraminifera Mg/Ca (temperature indicators) (Ziegler et al., 2010a, 2010b; Bunzel et al., 2017; Gebregiorgis et al., 2018; Stephanie et al., 2022).

Based on the new records of ISM variability from the eastern equatorial Indian Ocean, Bolton et al. (2013) showed that changes in upper water column structure and stratification in this region are dominated by wind-driven mixing. They use the planktic foraminiferal species *G. ruber* and *N. dutertrei*, recorders of upper mixed layer and thermocline conditions, respectively, to construct a new record ($\delta^{18}O_{G.\ ruber}$ minus $\delta^{18}O_{N.\ dutertrei}$, $\delta^{18}O_{r\text{-}d}$). Kim et al. (2018) considered that denitrification in the Arabian Sea is closely related to the monsoon-induced upwelling and subsequent phytoplankton production in the surface water. $\delta^{15}N$ values were high during interglacial periods, indicating intensified denitrification. These are an effective improvement and exploration of wind-based proxies. Unfortunately, these proxies still do not break the bounds of monsoon-driven productivity.

TABLE 1 A simplified summary of commonly used monsoon proxies in the region of India Monsoon.

	Features and processes	Proxies	Archives	Example	References
Wind-based proxies	Wind transport	grain size	Marine sediments	Arabian Sea	Clemens et al. (1996)
		Ti/Al ratio			Reichart et al. (1997); Sirocko et al. (2000)
		Pollen types and assemblages			Van Campo et al. (1982)
	Wind-driven upwelling	Upwelling-indicative phytoplankton and zooplankton, e.g., *G. bulloides*, *N. dutertrei*	Marine sediments	Arabian Sea	Clemens and Prell (1991); Anderson et al. (2002); Saraswat et al. (2019)
		Benthic foraminifera indicative of high carbon flux			den Dulk et al. (2000)
	Wind-induced structure of surface ocean	Geochemical proxies indicative of high productivity, e.g., C_{org}, opal, Ba, Ba/Al, $\delta^{15}N$, etc.	Marine sediments	Arabian Sea; Maldives	Clemens and Prell (2003); Ziegler et al. (2010b); Bunzel et al. (2017); Kim et al. (2018);
		Thermocline depth based on microfossils		Bay of Bengal	Bolton et al. (2013)
		planktonic foraminifera indicate SST (Mg/Ca)		Andaman Sea	Gebregiorgis et al. (2018)
Rain-based proxies	Precipitation	Speleothem $\delta^{18}O$	Cave speleothem	Indian subcontinent; Southwest China	Cai et al. (2010); Kotlia et al. (2015); Kathayat et al. (2016, 2017)
		$\delta^{13}C$ (C3/C4 plants)	Lacustrine deposits	Northern India	Kumar et al. (2022)
	Weathering and pedogenesis	Clay minerals	Hemipelagic sediments	Arabian Sea; Bay of Bengal	Thamban et al. (2002); Limmer et al. (2012); Joussain et al. (2016)
		Chemical weathering indices			Chen et al. (2020)
		Magnetic susceptibility	Marine sediments; Lacustrine sediments	Bay of Bengal; Heqing Basin	Weber et al. (2003)
		Magnetic grain size (ARM/SIRM ratio)			Xu et al. (2022)

On the other hand, rain-based proxies of chemical weathering in marine sediment have been used extensively. ISM, which accounts for the rainfall in Indian subcontinent can alter vegetational cover, runoff, erosion and weathering, and thus increase sediment transport to the Arabian Sea and the Bay of Bengal (Pandey et al., 2016; Clift, 2017), indicating a good coupling relationship between continental weathering/denudation and monsoon evolution (Thamban et al., 2002; Pandarinath, 2009; Das et al., 2013). The enhancement of the summer monsoon is accompanied by the increase of humidity index (such as kaolinite/chlorite and kaolinite/illite) and the increase of terrigenous detrital matter input (Thamban et al., 2002). The smectite/(illite + chlorite) has been confirmed to be ultimately forced by the intensity of chemical weathering in the source region associated with ISM variability (Cai et al., 2018). A number of weathering-related chemical proxies (e.g., CIA, α_K^{Al}, etc.), have also been applied to monsoon analysis at orbital timescales (Clift et al., 2014; Chen et al., 2020), with increased dominance of the ~100 kyr cycle. However, chemical weathering of source areas recorded in some marine sediments may also be influenced by factors such as temperature, rather than only ISM precipitation (An et al., 2011). In addition, the glacial-interglacial cycles lead to sea level fluctuations, such as the extensive exposure of marginal sea shelf during the glacial period, which may affect the spatial distribution pattern of precipitation in the provenance (Cai et al., 2015). Moreover, the changes of local ocean currents and shelf material transport in glacial-interglacial cycles may also lead to local environmental variations in marine sediments (Wang et al., 2014; Lu et al., 2020). Thus, how to effectively separate the temperature signals from the geological record of the summer monsoon is still worthy of further study. Fortunately, with the rapid development of speleothem paleoclimatology and highly precise dating technique of ^{230}Th in the last decade, the latest high-resolution rain-based proxies mainly from the cave speleothem of the Indian subcontinent and southwest China, are more widely used for paleoclimatic studies (Yuan et al., 2004; Wang et al., 2005; Cheng et al., 2009). At the orbital and millennium scales, speleothem $\delta^{18}O$ shows a relatively consistent variation throughout the Asian monsoon region (Fleitmann et al., 2003; Yuan et al., 2004; Wang et al., 2005; Cheng et al., 2006; Wang et al., 2008; Kotlia et al., 2015; Mishra et al., 2018), reflecting the circulation state in large space area and is a proxy of the ISM intensity from water vapor source to cave point (Kathayat et al., 2016, 2017). The stronger (weaker) ISM

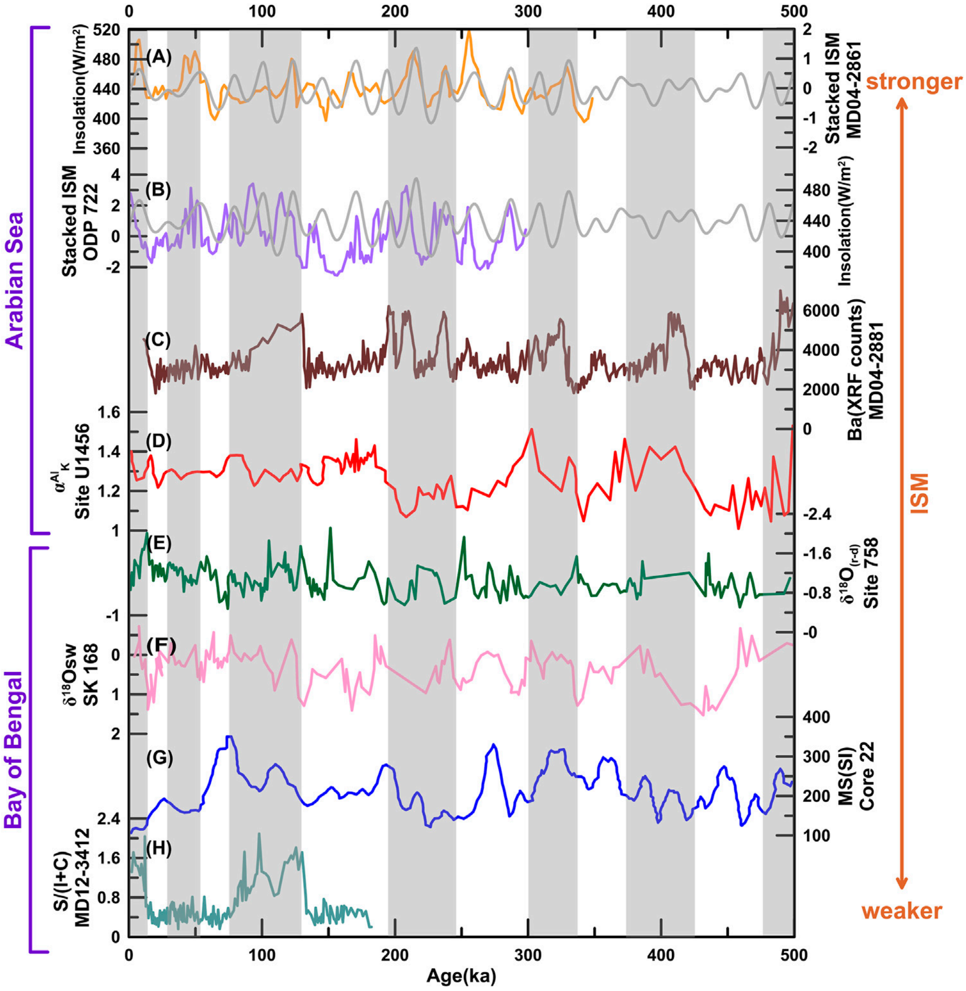

FIGURE 2
Comparison between the ISM records from marine sediments. **(A)** and **(B)** are the stacked ISM records from Arabian Sea cores MD04-2861 (Caley et al., 2011c) and ODP722 (Clemens and Prell, 2003), respectively. July 21 insolation at 65°N (grey) is plotted for comparison; **(C)** Ba counts record of MD04-2881 (Loulergue et al., 2008); **(D)** Variations in α_{K}^{Al} at Site U1456 (Chen et al., 2020); **(E)** Site 758 $\delta^{18}O_{(r-d)}$ record (Bolton et al., 2013); **(F)** Ice volume corrected δ^{18}Osw of SK 168 (Gebregiorgis et al., 2016); **(G)** Core 22 variation in Magnetic Susceptibility (MS) (Weber et al., 2003); **(H)** Temporal variations in Smectite/(Chlorite + Illite) (S/C + I) values (Joussain et al., 2016).

means that the cave has a higher ratio of water vapor from distant (near) source, showing a negative (positive) speleothem $\delta^{18}O$ (Yuan et al., 2004; Pausata et al., 2011; Kotlia et al., 2015). $\delta^{18}O$ variability in northern India is linked to periods of strong (weak) ISM circulation (Sinha et al., 2015). Strong (weak) ISM periods are characterized by enhanced (reduced) flux of isotopically depleted Bay of Bengal moisture and reduced (enhanced) flux of isotopically enriched Arabian Sea moisture (Sinha et al., 2015; Kaushal et al., 2018). As stalagmites are ultimately fed by rainwater, $\delta^{18}O$ reflects such changes in ISM circulation dynamics (Kaushal et al., 2018). The precession cycle of speleothem $\delta^{18}O$ series is obvious, which accords with the classical solar insolation driving theory of summer monsoon, and is also supported by the simulation results of different models (Liu et al., 2014; Tabor et al., 2018; Kutzbach et al., 2020). In addition, $\delta^{13}C$ values of lacustrine archive from India were used to determine the past plant (C3/C4 plants) variability driven by ISM (Amir et al., 2020; Kumar et al., 2022). Although it is relatively easy to obtain the samples, due to the limitation of the chronological sequence, it can only reflect the high resolution of millennial-scale variability.

It is remarkable that almost all new, high-resolution archives of paleo-monsoon variability are associated with precipitation rather than wind processes (Wang et al., 2014). However, the extent to which these proxies act as a strongly constrained indicator of summer monsoon intensity remains unclear.

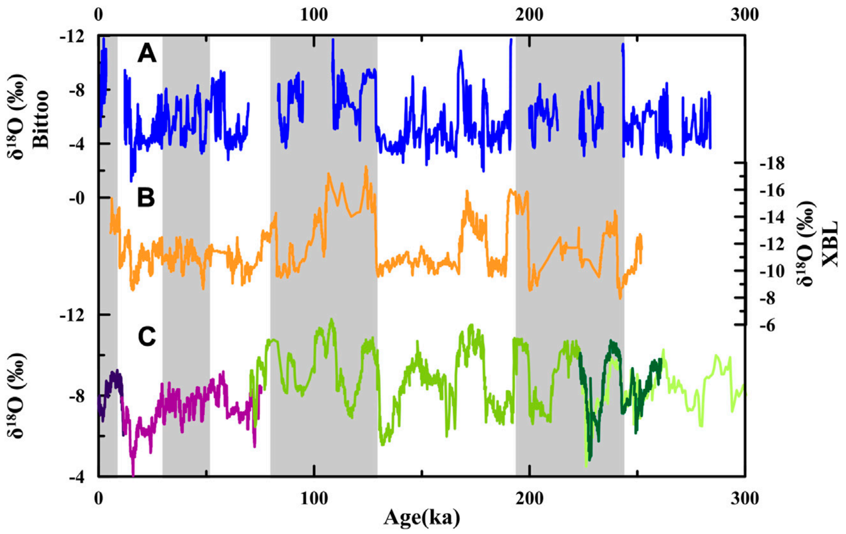

FIGURE 3
Comparison between the ISM records from cave speleothems. **(A)** $\delta^{18}O$ from Bittoo Caves (Kathayat et al., 2016); **(B)** $\delta^{18}O$ from Xiaobailong Cave (Cai et al., 2015); **(C)** $\delta^{18}O$ from Hulu Cave (purple) (Wang et al., 2001), Dongge Caves (dark blue) (Yuan et al., 2004), Sanbao Cave [light green (Wang et al., 2008), dark green (Cheng et al., 2009)] and Linzhu Cave (yellow-green) (Cheng et al., 2009).

2.2 Indian Monsoon variability since late quaternary

Since late Quaternary, many paleoclimate records show significant warming in the North Hemisphere and unconventionally stronger ISM (Yin and Guo, 2007; Ziegler et al., 2010a; Caley et al., 2011a). However, Ziegler et al. (2010b) conducted a comprehensive analysis of sediment record based on the core MD 04–2881, the high primary productivity in MIS 13 was not the result of an increase in the ISM, but of the strengthening of AMOC. The α_{K}^{Al} and smectite/(illite + chlorite) from IODP Site U1456 all indicate the enhancement of chemical weathering in provenance during MIS 13, confirming stronger ISM (Chen et al., 2020) (Figure 2). These interglacial periods (e.g., MIS 11, 9, and 5) are characterized by higher values of α_{K}^{Al} (Chen et al., 2020), further confirming the coupling between chemical weathering and ISM (Alizai et al., 2012; Cai et al., 2018). Those proxies ($\delta^{15}N$, grain size, Ba counts, Opal flux and *G. bulloides* %) of ISM indicate that the intensity of ISM increased firstly and reached a high value at about 300 ka, and then decreased during 300–250 ka (Clemens and Prell, 2003; Ziegler et al., 2010a; Gupta et al., 2010; Caley et al., 2011a). Saraswat et al. (2019) studied the $\delta^{18}O$ data of foraminifers in the eastern Arabian Sea over the past 350 ka, and observed an intense upwelling between MIS 7 (243–191 ka) and the early of MIS six caused by the intensification of ISM. To the late Pleistocene, the $\delta^{18}O$ records of two stalagmites from Tianmen Caves, the first cave records from the Tibetan Plateau, indicate the ISM strengthened significantly during MIS 5a, 5c, and 5e (Figure 3) (Cai et al., 2010, 2015). During warm sub-stages of MIS 5 (115–80 ka), the smectite/(illite + chlorite) maxima in the Bay of Bengal may be associated with intensification of ISM rainfall (Joussain et al., 2016). During 80–30 ka, the ISM intensity oscillated at intermediate levels between the Last Glacial Maximum (LGM) and Holocene (Kudrass et al., 2001). The LGM is characterized by high seawater $\delta^{18}O$ values, low gradient and low Ba/Ca which indicate the weaker ISM (Duplessy, 1982; Kudrass et al., 2001; Gebregiorgis et al., 2016). The proxy of humidity for sediments in the western continental margin of India indicates that the ISM in general was weaker during the late glaciation, with distinct events of intensification during 28–22 ka and 15.7–14.8 ka (Thamban et al., 2002). The depleted $\delta^{18}O$ values during early Holocene indicate the stronger ISM (Yuan et al., 2004; Cai et al., 2006; Dutt et al., 2015; Kathayat et al., 2016, 2017). Early to mid-Holocene ISM variability is characterized by a gradual intensification of monsoon rainfall (Rawat et al., 2012, 2015a, 2015b; Mishra et al., 2015a, 2015b; Gebregiorgis et al., 2016; Wang et al., 2020). The late Holocene witnessed a reduced rainfall activity and weak ISM (Thamban et al., 2002; Morrill et al., 2003; Dixit et al., 2014, 2018; Prasad et al., 2014, 2020; Dutt et al., 2018; Giesche et al., 2019; Phartiyal et al., 2020).

2.2.1 Orbital-scale variability

Solar insolation is the main external forcing factor of global climate change, and the interactions of the Earth's different layers modulated the amplitude and phase of climate response to solar insolation at different spatial and temporal scales through various physical, chemical and biological processes and feedback mechanisms (An et al., 2011; Wang et al., 2014; Wang et al., 2017). According to Milankovitch's astronomical climatology theory (Milankovitch, 1969), the periodic variation of solar radiation with latitude and season caused by changes in Earth's orbital parameters (eccentricity, obliquity and precession) is the fundamental driving force of climate change and ice age cycles at the 10^3–10^4 years scale. The influence of Earth orbital forcing on the long-term evolution of Indian monsoon has been recorded in deep-sea cores, lake sediments and stalagmites (Ziegler et al., 2010a; Cai et al., 2010; An et al., 2011). Previous researches demonstrated that the climate evolution of Indian monsoon is dominated by precession (~23 ka), obliquity (~41 ka) and eccentricity (~100 ka) cycles (e.g., Clemens et al., 1996; Clemens and Prell, 2003; Kelly et al., 2005; Kunkelova et al., 2018; Lindhorst et al., 2019; Lu et al., 2020).

Previous orbital-scale studies of the ISM mainly used proxies of phytoplankton (*G. bulloides*) from the northern Arabian Sea (Prell et al., 1984; Prell and Van Campo, 1986; Clemens and Prell, 1991), grain size (Clemens and Prell, 1990; Krissek and Clemens, 1992), Ti/Al and excess Ba MAR (Shimmield et al., 1990), biogenic opal and organic carbon MAR (Murray and Prell, 1991). In addition, various physical, chemical and biological parameters (e.g., dust flux, organic carbon content, planktonic and benthic foraminifera) are also used to indicate the intensity of ISM (Ziegler et al., 2010a, 2010b; Caley et al., 2011c; Bolton et al., 2013; Saraswat et al., 2019). Upwelling caused by the strong ISM controls marine primary productivity and contributes to the flourishing of unique plant and animal species in the northern Indian Ocean (e.g., *G. Bulloides* %). Productivity changes are associated with low-latitude processes in the Indian Ocean, independent of ice sheet growth and decline (Reichart et al., 1998; Beaufort et al., 2001). Information about monsoon variability and its seasonality is thus preserved in these marine biotas (e.g., planktonic and benthic foraminifera) (Ziegler et al., 2010a; Saraswat et al., 2019).

Comprehensive information on multiple proxies from marine sediments and terrestrial materials all indicate that ISM is dominated by a precession cycle in the long-term evolution (Clemens and Prell, 2003; Yuan et al., 2004; Cai et al., 2006, 2010, 2015; An et al., 2011; Dutt et al., 2015; Kathayat et al., 2016, 2017), and thus the ISM co-varies with the solar insolation in the Northern Hemisphere summer on the precession scale (e.g., Clemens and Prell, 2003; Clemens et al., 2008, 2010; Cai et al., 2010, 2015; Kathayat et al., 2016, 2017). However, solar insolation at low latitudes varies not only in precession cycles, but also in eccentricity and obliquity cycles. Clemens and Prell (2003) found that the obliquity and precession accounted for 26% and 18% of the variability of ISM, respectively, for the past 350 ka. Thus, it was proposed that obliquity is the driving force of the ISM rather than precession. A high-resolution record from Heqing Basin of southwestern China demonstrates that the Pleistocene ISM showed the orbital cycle signals of both eccentricity and precession. This may be because that the interhemispheric pressure gradient plays an important role in driving the ISM on glacial-interglacial cycles (An et al., 2011). The changes of clay mineral recorded in the Bay of Bengal and the eastern Arabian Sea since late Quaternary are relatively synchronous with the evolution of ISM, indicating that ISM is an important factor controlling weathering/erosion in South Asia on a millennium time scale (Thamban et al., 2002; Pandarinath, 2009; Das et al., 2013). Some proxies studied on the Bengal and India Fan provide palaeoclimatic evidence of monsoonal rainfall dynamics from provenance and their response to orbital forcing documented in the eccentricity (Chen et al., 2020; Lu et al., 2020) and obliquity band (Weber et al., 2018), but not obvious precession. The climate information recorded in marine sediments may be complicated due to the "Thermohaline Circulation" and the changes of nutrients in the glacial cycle caused by local ocean currents and the transport of shelf materials, and thus cannot display a pure precession cycle (Ziegler et al., 2010a; Lu et al., 2020). Unlike marine sediments, speleothem $\delta^{18}O$ provides a "fossil" record of rain, with relatively straightforward monsoon information (Wang et al., 2014; Wang et al., 2017).

In conclusion, the Indian monsoon may be controlled by many factors (e.g., AMOC, insolation, ice volume, and latent heat export, etc.). Different proxies for monsoon may provide conflicting understandings of the ISM evolution, leading to multiple points on the dynamic properties. Therefore, the combination of a variety of geological records and proxies is the key for a better understanding of the evolution and dynamics of the ISM on orbital-scale (e.g., Prell and Kutzbach, 1992; Clemens et al., 2008, 2010; Caley et al., 2011a, 2011b; Badesab et al., 2021; Rawat et al., 2021). Moreover, numerical simulation is also an indispensable method to verify the causal relationship between orbital forcing and ISM (Prell and Kutzbach, 1992; Kutzbach et al., 2008; Ziegler et al., 2010a, b).

2.2.2 Sub-orbital variations

The complexity of monsoon variability is also influenced by the high latitude climate to some extent, which is highlighted in the sub-orbital scale. Global monsoon variations in the sub-orbital scale are punctuated by a series of millennial-scale events (e.g., Heinrich, YD, Bølling/Allerød, etc.) at least over the past several glacial-interglacial cycles (Figure 4) (Demske et al., 2009; Paul et al., 2012; Rawat et al., 2012; Mishra et al., 2015; Cheng et al., 2016; Wang et al., 2017; Misra et al., 2019). These events have been recorded in speleothems, lake and marine sediments from the Indian monsoon affected areas (Miriyala et al., 2017; Bhushan et al., 2018; Gupta et al., 2021; Kumar et al., 2022), and it is consistent with the $\delta^{18}O$ record of Greenland ice cores (Yuan et al., 2004; Kelly et al., 2005). The variation of AMOC is also often used to explain millennial-scale monsoon events (Wang et al., 2008; Cheng et al., 2016). Likewise, speleothems in southern Tibetan plateau also record some ISM mutation events. Geochemical records of Cariaco Basin and the temperature record of Greenland during the early to mid-Holocene indicate that a

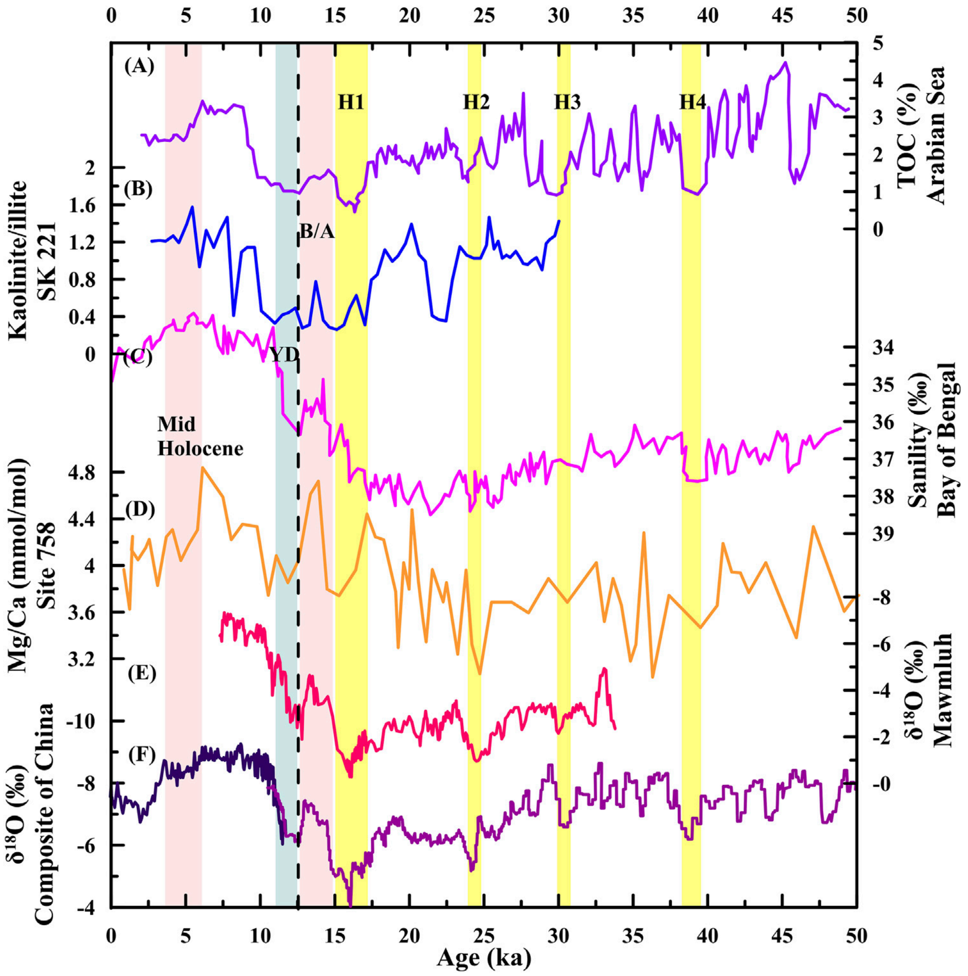

FIGURE 4
Comparison between high resolution ISM records. **(A)** Total organic carbon (TOC) content from Arabian Sea (Schulz et al., 1998); **(B)** Kaolinite to illite ratio from SK 221 in Arabian Sea (Das et al., 2013); **(C)** Salinity record from KL 126 in Bay of Bengal (Kudrass et al., 2001); **(D)** Mg/Ca record from Site 758 (Gebregiorgis et al., 2016); **(E)** δ^{18}O record from Mawnluh Cave (Dutt et al., 2015); **(F)** δ^{18}O records from Hulu Cave (Wang et al., 2001) and Dongge Cave (Yuan et al., 2004). Younger Dryas (YD), Bølling-Allerød (B/A), and Heinrich events (H1-4) are shaded based on stratigraphic boundaries defined by NGRIP (Andersen et al., 2006; Rasmussen et al., 2006).

relationship exists between the variability of ISM and high latitude climate at the millennium scale (Cai et al., 2012). Additionally, the climate change in the southern hemisphere also has an important influence on the Indian monsoon through trans-equatorial air flow and water vapor transport (Cai et al., 2006).

3 Precessional phase difference and its possible mechanisms

The controversy about the phase difference between the Indian monsoon variability and the NHSI in precession-band began in the early 1990s (Figure 5), which was first detected based on the monsoon upwelling tracer (*G. bulloides* %) correspond to the precession period, but with an 8 kyr phase lag relative to NHSI (Clemens et al., 1991). Later, the composite curve of ISM for the past 350 ka, based on other biological proxies (such as foraminifera assemblages, opal fluxes, etc.), further confirms the existence of this phase difference (Reichart et al., 1998; Clemens and Prell, 2003; Clemens et al., 2008, 2010). Therefore, it was deduced that the Indian monsoon is controlled not only by NHSI, but also by other factors, such as the thermal difference between the north and south hemisphere, ice sheets, etc. (Clemens et al., 1991, 2010; Clemens and Prell, 2003). The Indian monsoon water vapor cycle is accompanied by the release of latent heat from the southern Indian Ocean to the Indo-Asia. Thus, the release of latent heat may be the main mechanism of the ~8 ka lag of ISM in the precession-band (Clemens et al., 1991, 2010). However, the reliability of this phase difference is still disputed. The marine upwelling (or

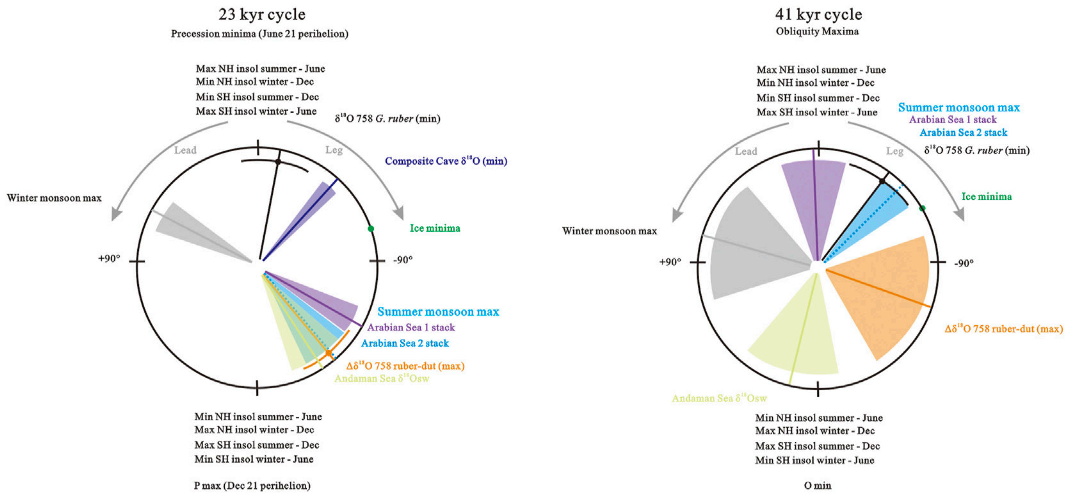

FIGURE 5
Phase wheels illustrating ISM response to orbital forcing. The precession index is defined as $\Delta\varepsilon\sin\omega$, where ω is the longitude of the perihelion measured from the moving vernal point and ε is the eccentricity of Earth's orbit about the sun (Laskar et al., 1993; Berger and Loutre, 1997). Obliquity is the axial tilt of Earth's rotation axis with respect to the orbital plane. In the phase wheel representation, the 12 o'clock position is set to precession minima (p min; $\omega = 90^\circ$, 21st June perihelion) obliquity maxima (O max), respectively. Negative/positive phases are measured in the clockwise/anticlockwise direction and represent phase lags/leads relative to p min or O max. Published records plotted (with shaded phase estimate errors) are the Arabian Sea summer monsoon stacks 1 (Clemens and Prell, 2003) and 2 (Caley et al., 2011c), composite cave $\delta^{18}O$ records from China (Cheng et al., 2009; Cai et al., 2015), corrected $\delta^{18}O_{sw}$ records from the Andaman Sea (Gebregiorgis et al., 2018), $\Delta\delta^{18}O$ records form Site 758 (Bolton et al., 2013), and winter and summer monsoon maxima (Clemens et al., 2008).

related indexes of productivity) in the Arabian Sea may be associated with the late phase of ISM in August-September, while the ~8 ka lag may be a response to this late summer insolation (Reichart et al., 1998). Therefore, it is believed that there is actually no phase difference between the insolation change caused by precession and the response of ISM. The ISM proxies used by Clemens et al. (2010) are not tightly coupled to the monsoon intensity. This so-called "phase difference" phenomenon may be affected by other geological processes (Ruddiman, 2006), e.g., the AMOC (Ziegler et al., 2010a), the breeze from the Arabian Sea (Conroy and Overpeck, 2011). The AMOC can control the nutrient transport in the euphotic zone of the Arabian Sea, and further influence the primary productivity and Oxygen Minimum Zones (OMZs) intensity. Therefore, it was deduced that AMOC dominates the precession lag of the maximum productivity in the Arabian Sea sediments (Ziegler et al., 2010a; 2010b), and the phase difference may not reflect the typical ISM records, but the breeze from the Arabian Sea (Conroy and Overpeck, 2011). Simulation results also confirmed the non-existence of the 8 kyr phase difference but a ~2 kyr lag between the ISM and the NHSI, which is consistent with the stalagmite $\delta^{18}O$ record in the Asian continent (Kutzbach et al., 2008).

In order to further verify this issue, the grain size proxy from the cores nearby, which is independent of the AMOC, was investigated and confirmed that the ISM proxies lag the NHSI by 9 ± 1 kyr in the precession-band (Caley et al., 2011b). Subsequently, this phase difference was also found in the sediments of the equatorial eastern Indian Ocean and the Andaman Sea. Bolton et al. (2013) proposed that the phase lag might reflect multiple forcing mechanisms, e.g., insolation, ice volume and latent heat export, based on the gradient of the $\delta^{18}O$ difference between two different foraminifera at ODP Site 758. Gebregiorgis et al. (2018) found this phase lag of 9 kyr in the Andaman Sea over the past 1 Ma, which implied that the NHSI may not be the major forcing for the ISM. However, this phenomenon has not been found in the sediments of the Bay of Bengal (Weber et al., 2018; Lauterbach et al., 2020). In the stalagmite records from the northern India and the southwest China, the ISM is almost contemporaneous with the NHSI without phase lag (Cai et al., 2010, 2015; Kathayat et al., 2016, 2017).

As a complex subsystem of the global monsoon, there must be "no real paradox" between the records of the ISM, whatever lands or seas. In the phase lag records of the Arabian Sea, the complexity caused by interaction of the African summer monsoon with the ISM may not be negligible. And in the southwest China, the relationship between the ISM and the EASM also needs to be considered. In addition, the role of Indian winter monsoon (northeast winds) is unclear. Therefore, different proxies (winds/rainfalls) may reflect different parts of the Indian monsoon system. With further research, it is time to reveal the real truth of this phase difference and to confirm its reliability and inherent mechanism(s) from a global perspective (An et al., 2011, 2015; Cheng et al., 2020).

4 Environmental magnetism contribution to monsoon investigations

4.1 Applications, advantages and limitations

Compared to other analyses (such as mineralogy and geochemistry), environmental magnetic method is rapid, easy, nondestructive, and cost-effective (Thompson and Oldfield, 1986; Evans and Heller, 2004). On Earth, the formation and transformation mechanisms of magnetic minerals are complex. Iron oxides, iron oxyhydroxides and iron sulfides can be converted into each other with many pathways (Dunlop and Özdemir, 1997; Michel et al., 2010; Jiang et al., 2022). The magnetic minerals in sediments and soils are sensitive to the formation environments (e.g., aridity/humidity, warm/cold) and transport process (e.g., wind, current). It is estimated that each iron atom in the sediments undergoes as many as 100 cycles of reduction and oxidation before being permanently buried (Thamdrup, 2000). Therefore, magnetic minerals are used to provide evidence for a wide range of environmental processes (Thompson and Oldfield, 1986; Evans and Heller, 2004; Liu et al., 2012). For example, hematite and goethite are formed under opposite climate conditions (dry and warm for hematite, wet and cool for goethite) and their formation processes are competitive (Schwertmann 1993). The presence and characteristics of goethite are indicators for soil-weathering conditions and burial history (Balsam et al., 2004). The hematite to (hematite + goethite) ratio [Hm/(Hm + Gt)] is controlled by the pedogenetic formation rate and depends primarily on the parent minerals, soil environment and the duration of pedogenesis (Cornell et al., 2003). Furthermore, the magnetofossil is an important source of fine magnetic minerals in sediments, with strong and stable magnetic properties, which can effectively record the changes of magnetotactic bacteria (MTB) ecological environment affected by climate (e.g., Hess, 1994; Snowball et al., 2002). In addition, the magnetic properties of the initial ferromagnetic minerals (e.g., magnetite and titanomagnetite) in the parent material actually determine the magnetic background values in the sediments dominated by detrital magnetic minerals. The later transport process may sort those magnetic particles, and the particle size decreases with the distance between source and depositional areas (Hatfield and Maher, 2009). During post-deposition, magnetic minerals may experience diagenetic process. In oxic environments, the most important diagenetic processes involve surface oxidation of detrital minerals (e.g., Torii, 1997; Liu et al., 2007; Chang et al., 2013), and precipitation of Fe(III)-bearing minerals from solution (e.g., Channell et al., 1982; Bouilloux et al., 2013). In ferruginous environments, the most reactive detrital and authigenic iron oxides undergo dissolution, often mediated by dissimilatory iron-reducing bacteria, which releases Fe(II) that becomes available for other reactions (Poulton et al., 2004; Roberts, 2015). In sulphidic environments, Hydrogen sulphide reacts with the Fe(II) released from iron mineral dissolution or directly with solid iron (oxyhydr-)oxide minerals to form iron sulphide minerals (Poulton et al., 2004; Roberts, 2015).

Those environmental magnetic parameters (e.g., magnetic susceptibility (χ), saturated isothermal remanence (SIRM), coercivity (B_c), SIRM/χ, ARM/SIRM, χ_{ARM}/χ, etc.) proxies of the concentration, mineralogy, and magnetic grain size, can reflect the environmental and climatic information recorded in the sediments (Thompson and Oldfield, 1986; Evans and Heller, 2004). In the early stage, only the contribution of a single magnetic susceptibility parameter was considered in the study of paleoclimate (Heller et al., 1993). With the deepening of research, more and more magnetic proxies have been proposed. In recent years, scholars added many kinds of characteristic information such as mineralogy and spectroscopy with magnetic parameters to quantitatively study the changes of paleo-precipitation and paleo-temperature (e.g., Balsam et al., 2011; Orgeira et al., 2011; Liu et al., 2013; Maxbauer et al., 2016). These quantitative methods, along with earlier more qualitative interpretations, hold enormous potential for understanding environmental variability in the deep past. Therefore, environmental magnetic method has been successfully used to assess the paleoclimate fluctuations recorded by loess/paleosol sequences, lacustrine and marine sediments (e.g., Deng et al., 2001; Liu et al., 2012; Ao et al., 2021; Liu et al., 2021). In particular, environmental magnetic parameters are used to reconstruct the Asian monsoon evolution successfully. For example, Nie et al. (2017) established an EASM record since the Late Miocene using the lacustrine sediments in the Qaidam Basin, northern China, which exhibits a dominant 100-ky periodicity similar to the EASM records during the Late Quaternary. Liu et al. (2021) showed that the environmental magnetic records from the Tengger Desert, China reveal wet–dry cycles at a dominant frequency of 405 kyr, with drier intervals corresponding to eccentricity minima. These findings are consistent with previous reconstructions of East Asian summer and North African summer monsoon precipitation variability. These results challenge the traditional view that high-latitude ice sheets are the primary driver of East Asian monsoon precipitation during the Quaternary based on Chinese loess records (Figure 6). In marine sediments, the variations of magnetic parameters are also widely used for establishing chronological framework, tracking provenances, current paths, and exploring global climate changes at orbital scale in the global marine sediments (e.g., Chang et al., 2016; Jiang and Liu, 2016; Yang et al., 2016).

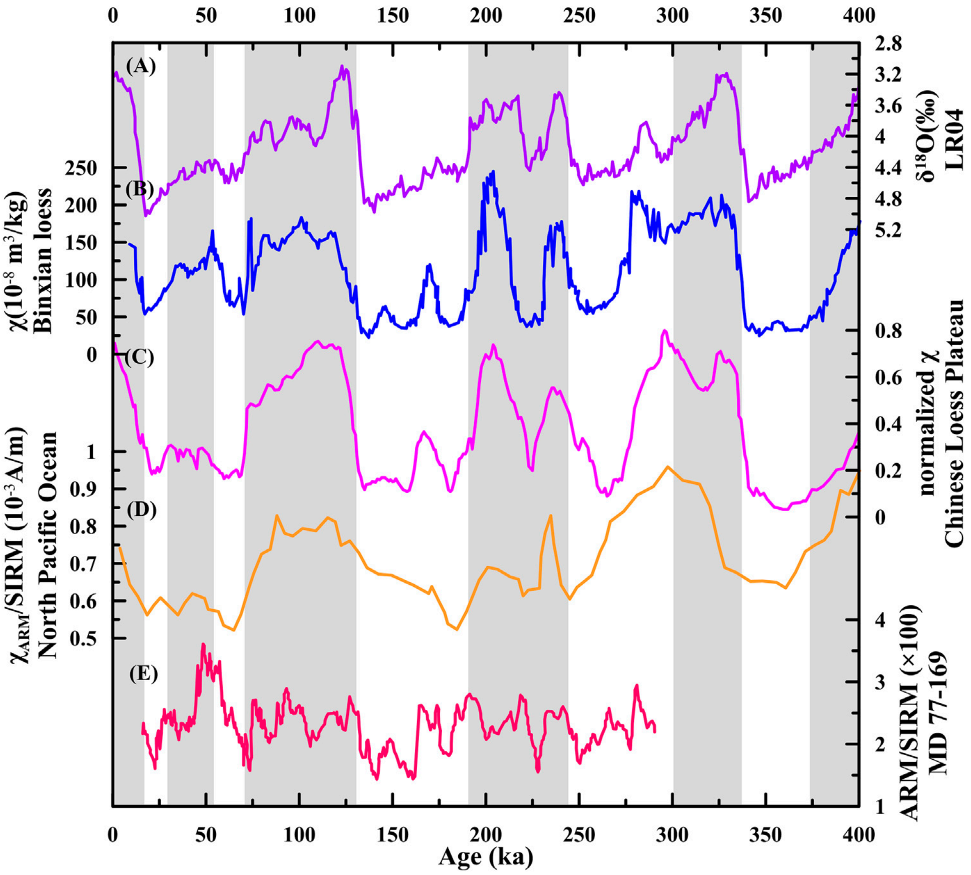

FIGURE 6
Paleo-monsoon records with environmental magnetism during the Late Quaternary. **(A)** Benthic LR04 $\delta^{18}O$ stack (Lisiecki and Raymo, 2005); **(B)** Binxian loess χ_{lf} records (Ao et al., 2020); **(C)** Normalized χ records from the Chinese Loess Plateau (Nie et al., 2017); **(D)** χ_{ARM}/SIRM records from core NGC65, North Pacific Ocean (Zhang et al., 2019); **(E)** ARM/SIRM records from core MD 77–169, the Andaman Sea (Colin et al., 1998).

In addition, several limitations should be considered when using environmental magnetic methods in paleoclimate studies. Firstly, the magnetic particles may still be mobile after deposition in the water-filled substrate. During this depositional process, the remanent magnetization will eventually be locked in at some depth. And this complex "lock-in" manner can cause some troubles for sediment dating by using magnetic method (Evans and Heller, 2004). Secondly, a single magnetic parameter (e.g., χ) may contain complex magnetic mineral information (e.g., components, contents, particles, etc.). It is crucial to select the suitable combination of parameters to separate the information for better understand its implications. Thirdly, different sediments compositions, provenances and post-deposition processes may result in the different interpretations for the magnetic parameters variability (Liu et al., 2012). Therefore, the transformation between different magnetic minerals should be considered for the environmental magnetic interpretation (Jiang et al., 2022). Therefore, more cautions are needed as using environmental magnetism for paleoclimatic studies.

4.2 Studies in the Indian Monsoon regions

In the Indian monsoon regions, although magnetic studies are relatively scarce, the environmental magnetic studies have still provided important evidence for the evolution of ISM. Phartiyal et al. (2003) established the climatic implications of the magnetic clusters and zones from Late Quaternary lacustrine sediments at Pithoragarh palaeolake, Kumaun Lesser Himalaya, India, with the correlations of pollen results. Kumar et al. (2020, 2021) first portrayed the moisture sources based on the high-resolution multi-proxy analyses (including environmental magnetism) from India and nearby regions. Their results indicated that the ISM controlled the glacier fluctuations in the Western Himalaya during Late Quaternary. A detailed magnetic analysis of ODP 722B demonstrated that fluctuations in the volume magnetic susceptibility was controlled by carbonate dilution, and the upper ferrimagnetic signal reflected the source area aridity (Hounslow and Maher, 1999). Magnetic susceptibility of the semi-abyssal sediments near the Bengal Fan decreased with the increase of $CaCO_3$ content, indicating the glacial-interglacial climate change, and the variation of magnetic susceptibility has 41 kyr cycles, which may be related to high-latitude forcing (Weber et al., 2003). Colin et al. (1998) studied the magnetic properties of cores MD77-169 and MD77-180 in the Andaman Sea and the Bay of Bengal, respectively, which shows a strong 23 kyr magnetic grain-size periodicity related to the chemical weathering driven by ISM rainfall in the past 280 ka. The magnetic grain size parameters (χ_{ARM}/SIRM, SIRM/χ_{LF}, χ_{ARM}/χ_{LF}) can track the variations of chemical weathering and ISM rainfall in the Andaman Sea. The fining of magnetic grain size manifests the associated intensification in chemical weathering during the strong ISM periods. While cold and dry periods are marked by an increase in magnetic grain size indicating the shift from chemical to physical weathering in the source regions (Sebastian et al., 2019). Badesab et al. (2021) evaluated the sedimentary (rock magnetic, sedimentological, mineralogical and inorganic geochemistry) records of the NGHP-01-17A core to elucidate the tectonic control on the sedimentation and diagenesis in the Andaman Sea over the past ~1 Ma. They proposed that rock magnetic properties effectively recorded the geological processes that controlled sedimentation over ~1 Ma in the Andaman Sea. In addition, A comparison of the GISP2 ice core isotopic record shows that rapid temperature variations (e.g., D-O, Heinrich and YD events) during the last glacial period, are also present in magnetic parameters, which reveals a remote correlation between the ISM and the North Atlantic climate (Colin et al., 1998; Li et al., 2006; Sebastian et al., 2019). Therefore, environmental magnetism is an indispensable method for further understanding the evolution of the ISM, especially in combination with other techniques (e.g., mineralogy, isotopic, geochemistry, sedimentology, and foraminiferal, etc.).

5 Conclusion and the way forward

Although a lot of work have been done on the Indian monsoon, there are still some deficiencies and disputes about the evolution of Indian Monsoon on orbital-scale since late Pleistocene, for example, whether the alternative indicators of monsoon in different sea areas can truly reflect the monsoon information? And what is the main forcing mechanism(s) for the phase difference between the Indian monsoon and NHSI? Specifically, at least some new work should be carried out in the following aspects.

1) More records from different regions. Records from different regions response to the Indian monsoon diversely. The ISM is characterized by strong winds and remarkable upwellings in the Arabian Sea, while it is characterized by heavy precipitations in the Bay of Bengal. In order to systematically study the evolution characteristics of the Indian monsoon, it is necessary to carry out systematic research in the Indian monsoon affecting regions. Previous studies mainly focused on the marginal sea of the Indian Ocean (e.g., Arabian Sea, Bay of Bengal, Andaman Sea, etc.) and the stalagmite records in the land monsoon regions. However, different conclusions were obtained, e.g., with 8 kyr phase lag in Arabian Sea sediments (Clemens et al., 1991, 2010; Clemens and Prell, 2003), and without phase lag in Bay of Bengal (Weber et al., 2018; Lauterbach et al., 2020). The equatorial Indian Ocean region is also affected by the Indian monsoon (Figure 1) (e.g., Tomczak and Godfrey, 2003; Betzler et al., 2013; Lüdmann et al., 2013; Bunzel et al., 2017; Alonso-Garcia et al., 2019), but there is a lack of discussion on the phase difference between ISM and NHSI. Therefore, in order to demonstrate whether this phase difference is unique to the sedimentary records of the Indian Ocean, it is necessary to find evidence in wider Indian monsoon control regions, especially in the equatorial Indian Ocean (e.g., Ninetyeast ridge and Maldives).

2) Evidence of other proxies. Most of the proxies used in the previous studies on this precession phase paradox are based on the relevant of marine primary productivity (e.g., planktonic foraminifera abundances, opal fluxes, etc.). There are few tests on physical parameters, especially on magnetism. Environmental Magnetism can trace the formations, transportations and post deposition processes of the magnetic minerals in sediments (Liu et al., 2012; Colombo et al., 2017; Jiang et al., 2022). It is widely used to study large-scale climate and environmental processes. A lot of environmental magnetism works have been carried out in the inner Asia (Deng et al., 2006; Nie et al., 2017; Ao et al., 2021; Liu et al., 2021), the Pacific Ocean (Zhang et al., 2019), the Japan Sea (Chang et al., 2016), the South China Sea (Yang et al., 2016; Li et al., 2018). The periodic evolution of East Asian Monsoon on different scales and its teleconnection with ice sheets also have been studied. In particular, the methods of environmental magnetism have provided important evidence for sediment provenances and evolutions of the Indian monsoon in the Bay of Bengal and the Andaman Sea. All these works provided a methodological basis for the paleoclimatic studies in the sediments of the Indian Ocean. Thus, the Environmental Magnetism is one of the effective methods to study the evolutions of Indian monsoon, which is hopeful to make contributions for the question of phase lag between ISM and NHSI.

3) The mechanism of phase difference. Many mechanisms have been proposed for the phase lag between the ISM variability and the NHSI, e.g., the cross equatorial latent heat transfer between the southern Indian Ocean and the Asian continent (Clemens et al., 1996; Clemens and Prell, 2003), the prolonged summer monsoon season related to higher insolation at the end of the summer (Reichart et al., 1998), or those summer monsoon proxies not tightly coupled with the monsoon intensity, but affected by other processes (Ruddiman, 2006; Ziegler et al., 2010a). Therefore, the mechanism of this time lag still needs more discussions.

Author contributions

LC, YG, LZ, and ZJ designed the study and wrote the paper. All authors provided significant input to the final manuscript.

Funding

This research was funded by the Marine S&T Fund of Shandong Province for Pilot National Laboratory for Marine Science and Technology (Qingdao) (No. 2022QNLM050302-5) and the National Natural Science Foundation of China (grants 41922026 and 4212005), the Fundamental Research Funds for the Central Universities (202072001 and 201941007), Taishan Scholars (ts20190918).

Conflict of interest

Publisher's note

References

Alizai, A., Hillier, S., Clift, P. D., Giosan, L., Hurst, A., VanLaningham, S., et al. (2012). Clay mineral variations in Holocene terrestrial sediments from the Indus Basin. *Quat. Res.* 77 (3), 368–381. doi:10.1016/j.yqres.2012.01.008

Alonso-Garcia, M., Rodrigues, T., Abrantes, F., Padilha, M., Alvarez-Zarikian, C. A., Kunkelova, T., et al. (2019). Sea-surface temperature, productivity and hydrological changes in the Northern Indian Ocean (Maldives) during the interval ~575-175 ka (MIS 14 to 7). *Palaeogeogr. Palaeoclimatol. Palaeoecol.* 536, 109376. doi:10.1016/j.palaeo.2019.109376

Amir, M., Paul, D., and Malik, J. N. (2020). Geochemistry of Holocene sediments from chilika lagoon, India: Inferences on the sources of organic matter and variability of the Indian summer monsoon. *Quat. Int.* 599-600, 148–157. doi:10.1016/j.quaint.2020.08.050

An, Z. S., Clemens, S. C., Shen, J., Qiang, X., Jin, Z., Sun, Y., et al. (2011). Glacial-interglacial Indian summer monsoon dynamics. *Science* 333, 719–723. doi:10.1126/science.1203752

An, Z. S., Kutzbach, J. E., Prell, W. L., and Porter, S. C. (2001). Evolution of Asian monsoons and phased uplift of the Himalaya-Tibetan plateau since Late Miocene times. *Nature* 411, 62–66. doi:10.1038/35075035

An, Z. S., Wu, G. X., Li, J. P., Sun, Y. B., Liu, Y. M., Zhou, W. J., et al. (2015). Global monsoon dynamics and climate change. *J. Earth Env.* 6 (6), 341–381. (In Chinese with English abstract). doi:10.7515/JEE201506001

Andersen, K. K., Svensson, A., Johnsen, S. J., Rasmussen, S. O., Bigler, M., Rothlisberger, R., et al. (2006). The Greenland ice core chronology 2005, 15-42 ka. Part 1: Constructing the time scale. *Quat. Sci. Rev.* 25 (23), 3246–3257. doi:10.1016/j.quascirev.2006.08.002

Anderson, D. M., Overpeck, J. T., and Gupta, A. K. (2002). Increase in the Asian Southwest monsoon during the past four centuries. *Science* 297, 596–599. doi:10.1126/science.1072881

Ao, H., Rohling, E. J., Zhang, R., Roberts, A. P., Holbourn, A. E., Ladant, J.-B., et al. (2021). Global warming-induced Asian hydrological climate transition across the Miocene-Pliocene boundary. *Nat. Commun.* 12 (1), 6935. doi:10.1038/s41467-021-27054-5

Ao, H., Rohling, E., Stringer, C., Roberts, A., Dekkers, M., Dupont-Nivet, G., et al. (2020). Two-stage mid-Brunhes climate transition and mid-Pleistocene human diversification. *Earth. Sci. Rev.* 210, 103354. doi:10.1016/j.earscirev.2020.103354

Badesab, F., Mascarenhas-Periera, M. B. L., Gaikwad, V., Dewangan, P., Panda, P. P., Deenadayalan, K., et al. (2021). Rock magnetic evidence of tectonic control on the sedimentation and diagenesis in the Andaman Sea over ~1 million years. *Mar. Pet. Geol.* 130, 105150. doi:10.1016/j.marpetgeo.2021.105150

Balsam, W. L., Ellwood, B. B., Ji, J. F., Williams, E. R., Long, X., and Hassani, A. E. (2011). Magnetic susceptibility as aproxy for rainfall: Worldwide data from tropical and temperate climate. *Quat. Sci. Rev.* 30 (19-20), 2732–2744. doi:10.1016/j.quascirev.2011.06.002

Balsam, W. L., Ji, J., and Chen, J. (2004). Climatic interpretation of the Luochuan and Lingtai loess sections, China, based on changing iron oxide mineralogy and magnetic susceptibility. *Earth planet. Sci. Lett.* 223, 335–348. doi:10.1016/j.epsl.2004.04.023

Beaufort, L., de Garidel-Thoron, T., Mix, A. C., and Pisias, N. G. (2001). ENSO-like forcing on oceanic primary production during the late Pleistocene. *Science* 293, 2440–2444. doi:10.1126/science.293.5539.2440

Berger, A., and Loutre, M. F. (1997). Inter tropical latitudes and precessional and half-precessional cycles. *Science* 278 (5342), 1476–1478. doi:10.1126/science.278.5342.1476

Betzler, C., Eberli, G., Kroon, D., Wright, J., Swart, P., Bejugam, N., et al. (2016). The abrupt onset of the modern South Asian Monsoon winds. *Sci. Rep.* 6, 29838. doi:10.1038/srep29838

Betzler, C., Eberli, G. P., Lüdmann, T., Reolid, J., Kroon, D., Reijmer, J. J. G., et al. (2018). Refinement of Miocene sea level and monsoon events from the sedimentary archive of the Maldives (Indian Ocean). *Prog. Earth Planet. Sci.* 5, 5. doi:10.1186/s40645-018-0165-x

Betzler, C., Lüdmann, L., Hübscher, C., and Fürstenauet, J. (2013). Current and sea-level signals in periplatform ooze (Neogene, Maldives, Indian Ocean). *Sediment. Geol.* 290, 126–137. doi:10.1016/j.sedgeo.2013.03.011

Bhushan, R., Sati, S. P., Rana, N., Shukla, A. D., Mazumdar, A. S., and Juyal, N. (2018). High-resolution millennial and centennial scale Holocene monsoon variability in the Higher Central Himalayas. *Palaeogeogr. Palaeoclimatol. Palaeoecol.* 489, 95–104. doi:10.1016/j.palaeo.2017.09.032

Bolton, C. T., Chang, L., Clemens, S. C., Kodama, K., Ikehara, M., Medina-Elizalde, M., et al. (2013). A 500, 000 year record of Indian summer monsoon dynamics recorded by eastern equatorial Indian Ocean upper water-column structure. *Quat. Sci. Rev.* 77, 167–180. doi:10.1016/j.quascirev.2013.07.031

Boos, W. R., and Kuang, Z. (2010). Dominant control of the South Asian monsoon by orographic insulation versus plateau heating. *Nature* 463 (7278), 218–222. doi:10.1038/nature08707

Bouilloux, A., Valet, J. P., Bassinot, F., Joron, J. L., Blanc-Valleron, M. M., Moreno, E., et al. (2013). Comprehensive plate models for the thermal evolution of oceanic lithosphere. *Geochem. Geophys. Geosyst.* 14, 3751–3778. doi:10.1002/ggge.20232

Bunzel, D., Schmiedl, G., Lindhorst, S., Mackensen, A., Reolid, J., Romahn, S., et al. (2017). A multi-proxy analysis of Late Quaternary ocean and climate variability for the Maldives, Inner Sea. *Clim. Past.* 13, 1791–1813. doi:10.5194/cp-13-1791-2017

Cai, M. J., Xu, Z. K., Clift, P. D., Khim, B.-K., Lim, D., Yu, Z., et al. (2018). Long-term history of sediment inputs to the eastern Arabian Sea and its implications for the evolution of the Indian summer monsoon since 3.7 Ma. *Geol. Mag.* 157 (6), 908–919. doi:10.1017/S0016756818000857

Cai, Y., Cheng, H., An, Z., Edwards, R. L., Wang, X., Tan, L., et al. (2010). Large variations of oxygen isotopes in precipitation over south-central Tibet during Marine Isotope Stage 5. *Geology* 38 (3), 243–246. doi:10.1130/G30306.1

Cai, Y., Fung, I. Y., Edwards, R. L., An, Z., Cheng, H., Lee, J.-E., et al. (2015). Variability of stalagmite-inferred Indian monsoon precipitation over the past 252, 000 y. *Proc. Natl. Acad. Sci. U. S. A.* 112 (10), 2954–2959. doi:10.1073/pnas.1424035112

Cai, Y. J., An, Z. S., Cheng, H., Edwards, R. L., Kelly, M. J., Liu, W., et al. (2006). High-resolution absolute-dated Indian monsoon record between 53 and 36 ka from Xiaobailong Cave, southwestern China. *Geol.* 34 (8), 621–624. doi:10.1130/G22567.1

Cai, Y., Zhang, H., Cheng, H., An, Z., Edwards, R., Wang, X., et al. (2012). The Holocene Indian monsoon variability over the southern Tibetan Plateau and its teleconnections. *Earth Planet. Sci. Lett.* 335-336, 135–144. doi:10.1016/j.epsl.2012.04.035

Caley, T., Malaizé, B., Bassinot, F., Clemens, S. C., Caillon, N., Rossignol, L., et al. (2011c). The monsoon imprint during the ‘atypical’ MIS 13 as seen through north and equatorial Indian Ocean records. *Quat. Res.* 76, 285–293. doi:10.1016/j.yqres.2011.07.001

Caley, T., Malaizé, B., Revel, M., Ducassou, E., Wainer, K., Ibrahim, M., et al. (2011a). Orbital timing of the Indian, East Asian and African boreal monsoons and the concept of a ‘global monsoon. *Quat. Sci. Rev.* 30 (25-26), 3705–3715. doi:10.1016/j.quascirev.2011.09.015

Caley, T., Malaizé, B., Zaragosi, S., Rossignol, L., Bourget, J., Eynaud, F., et al. (2011b). New Arabian Sea records help decipher orbital timing of Indo-Asian monsoon. *Earth Planet. Sci. Lett.* 308 (3-4), 433–444. doi:10.1016/j.epsl.2011.06.019

Chang, L., Bolton, C. T., Dekkers, M. J., Hayashida, A., Heslop, D., Krijgsman, W., et al. (2016). Asian monsoon modulation of nonsteady state diagenesis in hemipelagic marine sediments offshore of Japan. *Geochem. Geophys. Geosyst.* 17 (11), 4383–4398. doi:10.1002/2016gc006344

Chang, L., Winklhofer, M., Roberts, A. P., Heslop, D., Florindo, F., Dekkers, M. J., et al. (2013). Low-temperature magnetic properties of pelagic carbonates: Oxidation of biogenic magnetite and identification of magnetosome chains. *J. Geophys. Res. Solid Earth* 118, 6049–6065. doi:10.1002/2013JB010381

Channell, J. E. T., Freeman, R., Heller, F., and Lowrie, W. (1982). Timing of diagenetic haematite growth in red pelagic limestones from Gubbio (Italy). *Earth Planet. Sci. Lett.* 58, 189–201. doi:10.1016/0012-821X(82)90193-5

Chen, G.-S., Liu, Z., and Kutzbach, J. E. (2014). Reexamining the barrier effect of the Tibetan Plateau on the South Asian summer monsoon. *Clim. Past.* 10, 1269–1275. doi:10.5194/cp-10-1269-2014

Chen, H., Xu, Z., Lim, D., Clift, P. D., Chang, F., Li, T., et al. (2020). Geochemical records of the provenance and silicate weathering/erosion from the eastern Arabian Sea and their responses to the Indian summer monsoon since the Mid-Pleistocene. *Paleoceanogr. Paleoclimatol.* 35, e2019PA003732. doi:10.1029/2019PA003732

Cheng, H., Edwards, R. L., Broecker, W. S., Denton, G. H., Kong, X., Wang, Y., et al. (2009). Ice age terminations. *Science* 326, 248–252. doi:10.1126/science.1177840

Cheng, H., Edwards, R. L., Sinha, A., Spötl, C., Yi, L., Chen, S., et al. (2016). The Asian monsoon over the past 640, 000 years and ice age terminations. *Nature* 534, 640–646. doi:10.1038/nature18591

Cheng, H., Edwards, R. L., Wan, Y. J., Ko, X. G., Ming, Y. F., Kelly, M. J., et al. (2006). A penultimate glacial monsoon record from Hulu Cave and two-phase glacial terminations. *Geol.* 34, 217–220. doi:10.1130/G22289.1

Cheng, H., Li, H., Zhang, X., Zhang, H., Yi, L., Cai, Y., et al. (2020). European-Asian-african continent: An early form of supercontinent and supermonsoon. *Quat. Sci.* 40 (6), 1381–1396. (In Chinese with English abstract). doi:10.11928/j.issn.1001-7410.2020.06.01

Cheng, H., Sinha, A., Wang, X., Cruz, F. W., and Edwards, R. L. (2012). The global paleomonsoon as seen through speleothem records from Asia and the Americas. *Clim. Dyn.* 39, 1045–1062. doi:10.1007/s00382-012-1363-7

Cheng, H., Zhang, H., Cai, Y., Shi, Z., Yi, L., Deng, C., et al. (2021). Orbital-scale Asian summer monsoon variations: Paradox and exploration. *Sci. China Earth Sci.* 64 (4), 529–544. doi:10.1007/S11430-020-9720-Y

Cheng, H., Zhang, H., Zhao, J., Li, H., Ning, Y., and Kathayat, G. (2019). Chinese stalagmite paleoclimate researches: A review and perspective. *Sci. China Earth Sci.* 62, 1489–1513. doi:10.1007/s11430-019-9478-3

Clemens, S. C., Murray, D. W., and Prell, W. L. (1996). Nonstationary phase of the pliopleistocene asian monsoon. *Science* 274, 943–948. doi:10.1126/science.274.5289.943

Clemens, S. C., and Prell, W. L. (2003). A 350, 000 year summer-monsoon multi-proxy stack from the owen ridge, northern Arabian Sea. *Mar. Geol.* 201 (1-3), 35–51. doi:10.1016/S0025-3227(03)00207-X

Clemens, S. C., and Prell, W. L. (1991). Late quaternary forcing of Indian ocean summer-monsoon winds: A comparison of fourier model and general circulation model results. *J. Geophys. Res.* 96 (22), 22683–22700. doi:10.1029/91JD02205

Clemens, S. C., Prell, W. L., Sun, Y., Liu, Z., and Chen, G. (2008). Southern hemisphere forcing of pliocene δ^{18}O and the evolution of indo-asian monsoons. *Paleoceanography* 3, PA4210. doi:10.1029/2008PA001638

Clemens, S. C., Prell, W. L., and Sun, Y. (2010). Orbital-scale timing and mechanisms driving Late Pleistocene Indo-Asian summer monsoons: Reinterpreting cave speleothem δ^{18}O. *Paleoceanography* 25, PA4207. doi:10.1029/2010PA001926

Clemens, S. C., and Prell, W. L. (2007). The timing of orbital-scale Indian monsoon changes. *Quat. Sci. Rev.* 26 (3-4), 275–278. doi:10.1016/j.quascirev.2006.11.010

Clemens, S., and Prell, W. L. (1990). Late Pleistocene variability of Arabian Sea summer monsoon winds and continental aridity: Eolian records from the lithogenic component of deep-sea sediments. *Paleoceanography* 5, 109–145. doi:10.1029/PA005i002p00109

Clemens, S., Prell, W., Murray, D., Shimmield, G., and Weedon, G. (1991). Forcing mechanisms of the Indian Ocean monsoon. *Nature* 353 (6346), 720–725. doi:10.1038/353720a0

Clift, P. D. (2017). Cenozoic sedimentary records of climate-tectonic coupling in the Western Himalaya. *Prog. Earth Planet. Sci.* 4, 39. doi:10.1186/s40645-017-0151-8

Clift, P. D., Hodges, K. V., Heslop, D., Hannigan, R., Van Long, H., and Calves, G. (2008). Correlation of Himalayan exhumation rates and Asian monsoon intensity. *Nat. Geosci.* 1, 875–880. doi:10.1038/ngeo351

Clift, P. D., Wan, S., and Blusztajn, J. (2014). Reconstructing chemical weathering, physical erosion and monsoon intensity since 25 Ma in the northern south China sea: A review of competing proxies. *Earth. Sci. Rev.* 130, 86–102. doi:10.1016/j.earscirev.2014.01.002

Colin, C., Kissel, C., Blamart, D., and Turpin, L. (1998). Magnetic properties of sediments in the Bay of bengal and the Andaman Sea: Impact of rapid North Atlantic ocean climatic events on the strength of the Indian monsoon. *Earth Planet. Sci. Lett.* 160 (3), 623–635. doi:10.1016/S0012-821X(98)00116-2

Colombo, C., Iorio, E. D., Liu, Q., Jiang, Z., and Barrón, V. (2017). Iron oxide nanoparticles in soils: Environmental and agronomic importance. *J. Nanosci. Nanotechnol.* 17 (7), 761–4460. doi:10.1166/jnn.2018.15294

Conroy, J. L., and Overpeck, J. T. (2011). Regionalization of present-day precipitation in the greater monsoon region of Asia. *J. Clim.* 24, 4073–4095. doi:10.1175/2011JCLI4033.1

Cornell, R., and Schwertmann, U. (2003). *The iron oxides*. New York: VCH Weinheim.

da Costa, G. M., Van San, E., De Grave, E., Vandenberghe, R. E., Barrón, V., and Datas, L. (2002). Al hematites prepared by homogeneous precipitation of oxinates: Material characterization and determination of the morin transition. *Phys. Chem. Min.* 29, 122–131. doi:10.1007/s002690100201

Das, S. S., Rai, A. K., Akaram, V., Verma, D., Pandey, A. C., Dutta, K., et al. (2013). Paleoenvironmental significance of clay mineral assemblages in the southeastern Arabian Sea during last 30 kyr. *J. Earth Syst. Sci.* 122 (1), 173–185. doi:10.1007/s12040-012-0251-1

Deeken, A., Thiede, R. C., Sobel, E. R., Hourigan, J. K., and Strecker, M. R. (2011). Exhumational variability within the Himalaya of northwest India. *Earth Planet. Sci. Lett.* 1–2, 103–114. doi:10.1016/j.epsl.2011.02.045

Demske, D., Tarasov, P. E., Wünnemann, B., and Riedel, F. (2009). Late glacial and Holocene vegetation, Indian monsoon and westerly circulation in the Trans-Himalaya recorded in the lacustrine pollen sequence from Tso Kar, Ladakh, NW India. *Palaeogeogr. Palaeoclimatol. Palaeoecol.* 279, 172–185. doi:10.1016/j.palaeo.2009.05.008

den Dulk, M., Reichart, G. J., van Heyst, S., Zachariasse, W. J., and van den Zwaan, G. J. (2000). Benthic foraminifera as proxies of organic matter flux and bottom water oxygenation? Acase history from the northern Arabian Sea. *Palaeogeogr. Palaeoclimatol. Palaeoecol.* 161, 337–359. doi:10.1016/S0031-0182(00)00074-2

Deng, C., Shaw, J., Liu, Q., Pan, Y., and Zhu, R. (2006). Mineral magnetic variation of the Jingbian loess/paleosol sequence in the northern Loess Plateau of China: Implications for Quaternary development of Asian aridification and cooling. *Earth Planet. Sci. Lett.* 241 (1), 248–259. doi:10.1016/j.epsl.2005.10.020

Deng, C., Zhu, R., Jackson, M. J., Verosub, K. L., and Singer, M. J. (2001). Variability of the temperature-dependent susceptibility of the Holocene eolian deposits in the Chinese Loess Plateau: A pedogenesis indicator. *Phys. Chem. Earth Part A Solid Earth Geodesy* 26 (11-12), 873–878. doi:10.1016/S1464-1895(01)00135-1

Dixit, Y., Hodell, D. A., Giesche, A., Tandon, S. K., Gazquez, F., Saini, H. S., et al. (2018). Intensified summer monsoon and the urbanization of Indus Civilization in northwest India. *Sci. Rep.* 8, 4225. doi:10.1038/s41598-018-22504-5

Dixit, Y., Hodell, D. A., and Petrie, C. A. (2014). Abrupt weakening of the summer monsoon in northwest India 4100 yr ago. *Geology* 42, 339–342. doi:10.1130/G35236.1

Dunlop, D. J., and Özdemir, Ö. (1997). *Rock magnetism: Fundamentals and frontiers*. Cambridge University Press.

Duplessy, J. (1982). Glacial to interglacial contrasts in the northern Indian Ocean. *Nature* 295, 494–498. doi:10.1038/295494a0

Dutt, S., Gupta, A. K., Clemens, S. C., Cheng, H., Singh, R. K., Kathayat, G., et al. (2015). Abrupt changes in Indian summer monsoon strength during 33, 800 to 5500 years B.P. *Geophys. Res. Lett.* 42, 5526–5532. doi:10.1002/2015GL064015

Dutt, S., Gupta, A. K., Wünnemann, B., and Yan, D. (2018). A long arid interlude in the Indian summer monsoon during~ 4, 350 to 3, 450 cal. yr BP contemporaneous to displacement of the Indus valley civilization. *Quat. Int.* 482, 83–92. doi:10.1016/j.quaint.2018.04.005

Evans, M. E., and Heller, F. (2004). Environmental magnetism: Principles and applications of enviromagnetics. *Quat. Sci. Rev.* 23 (16), 1867–1868. doi:10.1016/j.quascirev.2004.05.004

Fleitmann, D., Burns, S. J., Mudelsee, M., Neff, U., Kramers, J., Mangini, A., et al. (2003). Holocene forcing of the Indian monsoon recorded in a stalagmite from southern Oman. *Science* 300 (5626), 1737–1739. doi:10.1126/science.1083130

Gebregiorgis, D., Hathorne, E. C., Giosan, L., Clemens, S., Nürnberg, D., and Frank, M. (2018). Southern Hemisphere forcing of South Asian monsoon precipitation over the past ~1 million years. *Nat. Commun.* 9 (1), 4702–4708. doi:10.1038/s41467-018-07076-2

Gebregiorgis, D., Hathorne, E. C., Sijinkumar, A. V., Nath, B. N., Nürnberg, D., and Frank, M. (2016). South Asian summer monsoon variability during the last ~54 kyrs inferred from surface water salinity and river runoff proxies. *Quat. Sci. Rev.* 138, 6–15. doi:10.1016/j.quascirev.2016.02.012

Giesche, A., Staubwasser, M., Petrie, C. A., and Hodell, D. A. (2019). Indian winter and summer monsoon strength over the 4.2 ka BP event in foraminifer isotope records from the Indus River delta in the Arabian Sea. *Clim. Past.* 15, 73–90. doi:10.5194/cp-15-73-2019

Gupta, A. K., and Anderson, D. M. (2005). Mysteries of the Indian Ocean monsoon system. *J. Geol. Soc. India* 65 (1), 54–60.

Gupta, A. K., Sarkar, S., De, S., Clemens, S., and Velu, A. (2010). Mid-Brunhes strengthening of the Indian Ocean Dipole caused increased equatorial East African and decreased Australasian rainfall. *Geophys. Res. Lett.* 37 (6), L06706. doi:10.1029/2009GL042225

Gupta, A. K., Singh, R. K., Dutt, S., Cheng, H., Clemens, S. C., and Kathayat, G. (2021). High-frequency shifts in the Indian summer monsoon following termination of the YD event. *Quat. Sci. Rev.* 259 (1), 106888. doi:10.1016/J.QUASCIREV.2021.106888

Hao, Q., Zhang, R., Wang, P., and Wang, B. (2016). Monsoons across multi-scales: Summary of fourth conference on earth system science. *Adv. Earth Sci.* 31 (7), 689–699. (In Chinese with English abstract). doi:10.11867/j.issn.1001-8166.2016.07.0689

Hatfield, R. G., and Maher, B. A. (2009). Fingerprinting upland sediment sources: Particle size-specific magnetic linkages between soils, lake sediments and suspended sediments. *Earth Surf. Process. Landf.* 34 (10), 1359–1373. doi:10.1002/esp.1824

Heller, F., Shen, C. D., Beer, J., Liu, X. M., Liu, T. S., Bronger, A., et al. (1993). Quantitative estimates of pedogenic ferromagnetic mineral formation in Chinese loess and palaeoclimatic implications. *Earth planet. Sci. Lett.* 114 (2-3), 385–390. doi:10.1016/0012-821X(93)90038-B

Hess, P. P. (1994). Evidence for bacterial paleoecological origin of mineral magnetic cycles in oxic and sub-oxic Tasman Sea sediments. *Mar. Geol.* 117, 1~17. doi:10.1016/0025-3227(94)90003-5

Hounslow, M. W., and Maher, B. A. (1999). Source of the climate signal recorded by magnetic susceptibility variations in Indian Ocean sediments. *J. Geophys. Res.* 104 (B3), 5047–5061. doi:10.1029/1998JB900085

Jian, Z., Huang, B., Kuhnt, W., and Lin, H.-L. (2001). Late quaternary upwelling intensity and East Asian monsoon forcing in the south China sea. *Quat. Res.* 55, 363–370. doi:10.1006/qres.2001.2231

Jiang, Z., and Liu, Q. (2016). Quantification of hematite and its climatic significances. *Quat. Sci.* 36 (3), 676–689. (In Chinese with English abstract). doi:10.11928/j.issn.1001-7410.2016.03.17

Jiang, Z., Liu, Q., Roberts, A. P., Dekkers, M. J., Barrón, V., Torrent, J., et al. (2022). The magnetic and color reflectance properties of hematite: From earth to mars. *Rev. Geophys.* 60, e2020RG000698. doi:10.1029/2020RG000698

Joussain, R., Colin, C., Liu, Z., Meynadier, L., Fournier, L., Fauquembergue, K., et al. (2016). Climatic control of sediment transport from the Himalayas to the proximal NE Bengal Fan during the last glacial-interglacial cycle. *Quat. Sci. Rev.* 148, 1–16. doi:10.1016/j.quascirev.2016.06.016

Kathayat, G., Cheng, H., Sinha, A., Spötl, C., Edwards, R. L., Zhang, H., et al. (2016). Indian monsoon variability on millennial-orbital timescales. *Sci. Rep.* 6 (1), 24374–24377. doi:10.1038/srep24374

Kathayat, G., Cheng, H., Sinha, A., Yi, L., Li, X., Zhang, H., et al. (2017). The Indian monsoon variability and civilization changes in the Indian subcontinent. *Sci. Adv.* 3, e1701296. doi:10.1126/sciadv.1701296

Kaushal, N., Breitenbach, S. F. M., Lechleitner, F. A., Sinha, A., Tewari, V. C., Ahmad, S. M., et al. (2018). The Indian summer monsoon from a speleothem δ^{18}O perspective—a review. *Quaternary* 1, 29. doi:10.3390/quat1030029

Kelly, M. J., Edwards, R. L., Cheng, H., Yuan, D., Cai, Y., Zhang, M., et al. (2005). High resolution characterization of the Asian Monsoon between 146, 000 and 99, 000 years BP from Dongge Cave, China and global correlation of events surrounding Termination II. *Palaeogeogr. Palaeoclimatol. Palaeoecol.* 236, 20–38. doi:10.1016/j.palaeo.2005.11.042

Kim, J. E., Khim, B., Ikehara, M., and Lee, J. (2018). Orbital-scale denitrification changes in the Eastern Arabian Sea during the last 800 kyrs. *Sci. Rep.* 8 (1), 7027. doi:10.1038/s41598-018-25415-7

Kotlia, B. S., Singh, A. K., Joshi, L. M., and Dhaila, B. S. (2015). Precipitation variability in the Indian central Himalaya during last ca. 4, 000 years inferred from a speleothem record: Impact of Indian summer monsoon (ISM) and westerlies. *Quat. Int.* 371, 244–253. doi:10.1016/j.quaint.2014.10.066

Krissek, L. A., and Clemens, S. C. (1992). Evidence for aridity-driven dust flux to the northwest Arabian Sea and for decoupling of the dust and upwelling systems. *Spec. Publ.-Geol. Soc. Lond.* 64, 359–378. doi:10.1144/gsl.sp.1992.064.01.24

Kroon, D., and Ganssen, G. (1989). Northern Indian Ocean upwelling cells and the stable isotope composition of living planktonic foraminifers. *Deep Sea Res. Part A. Oceanogr. Res. Pap.* 36, 1219–1236. doi:10.1016/0198-0149(89)90102-7

Kroon, D., Steens, T., and Troelstra, S. (1991). Onset of monsoonal related upwelling in the western Arabian Sea as revealed by planktonic foraminifers. *Proc. Ocean. Drill. Program Sci. Results* 117, 257–263. doi:10.2973/odp.proc.sr.117.126.1991

Kudrass, H. R., Hofmann, A., Doose, H., Emeis, K., and Erlenkeuser, H. (2001). Modulation and amplification of climatic changes in the Northern Hemisphere by the Indian summer monsoon during the past 80 k.y. *Geol.* 29, 63–66. doi:10.1130/0091-7613(2001)029<0063:maaocc>2.0.co;2

Kumar, M., Saikia, K., Agrawal, S., Ghosh, R., Ali, S. N., Arif, M., et al. (2022). Climatic control on the C3 and C4 plant abundance during the late Pleistocene-Holocene in the northern Gangetic Plain, India. *Palaeogeogr. Palaeoclimatol. Palaeoecol.* 591, 110890. doi:10.1016/J.PALAEO.2022.110890

Kumar, O., Ramanathan, A. L., Bakke, J., Kotlia, B. S., and Shrivastava, J. P. (2020). Disentangling source of moisture driving glacier dynamics and identification of 8.2 ka event: Evidence from pore water isotopes, western Himalaya. *Sci. Rep.* 10 (1), 15324. doi:10.1038/s41598-020-71686-4

Kumar, O., Ramanathan, A. L., Bakke, J., Kotlia, B. S., Shrivastava, J. P., Kumar, P., et al. (2021). Role of Indian summer monsoon and westerlies on glacier variability in the Himalaya and East Africa during late quaternary: Review and new data. *Earth. Sci. Rev.* 212, 103431. doi:10.1016/j.earscirev.2020.103431

Kunkelova, T., Jung, S. J. A., de Leau, E. S., Odling, N., Thomas, A. L., Betzler, C., et al. (2018). A two million year record of low-latitude aridity linked to continental weathering from the Maldives. *Prog. Earth Planet. Sci.* 5, 86. doi:10.1186/s40645-018-0238-x

Kutzbach, J. E., Guan, J., He, F., Cohen, A. S., Orland, I. J., and Chen, G. (2020). African climate response to orbital and glacial forcing in 140, 000-y simulation with implications for early modern human environments. *Proc. Natl. Acad. Sci. U. S. A.* 117, 2255–2264. doi:10.1073/pnas.1917673117

Kutzbach, J. E. (1981). Monsoon climate of the early Holocene: Climate experiment with the Earth's orbital parameters for 9000 years ago. *Science* 214 (4516), 59–61. doi:10.1126/science.214.4516.59

Kutzbach, J., Liu, X., Liu, Z., and Chen, G. (2008). Simulation of the evolutionary response of global summer monsoons to orbital forcing over the past 280, 000 years. *Clim. Dyn.* 30 (6), 567–579. doi:10.1007/s00382-007-0308-z

Laskar, J., Joutel, F., and Boudin, F. (1993). Orbital, precessional, and insolation quantities for the Earth from -20 Myr to +10 Myr. *Astron. Astrophys.* 270, 522–533. doi:10.1086/116505

Lauterbach, S., Andersen, N., Wang, Y. V., Blanz, T., Larsen, T., and Schneider, R. R. (2020). An ~130 kyr record of surface water temperature and δ^{18}O from the northern Bay of bengal: Investigating the linkage between Heinrich events and weak monsoon intervals in Asia. *Paleoceanogr. Paleoclimatol.* 35 (2), e2019PA003646. doi:10.1029/2019PA003646

Li, H., Zhang, S., Fang, N., and Wang, H. (2006). Magnetic records of Core MD77-181 in the Bay of Bengal and their paleoenvironmental implications. *Chin. Sci. Bull.* 51, 1884–1893. doi:10.1007/s11434-006-2057-5

Li, J., Yue, L., Pan, F., Zhang, R., Guo, Lin, Xi, R., et al. (2014). Intensified aridity of the Asian interior recorded by the magnetism of red clay in Altun Shan, NE Tibetan Plateau. *Palaeogeogr. Palaeoclimatol. Palaeoecol.* 411, 30–41. doi:10.1016/j.palaeo.2014.06.017

Li, M., Ouyang, T., Roberts, A. P., Heslop, D., Zhu, Z., Zhao, X., et al. (2018). Influence of sea level change and centennial East Asian monsoon variations on northern south China Sea sediments over the past 36 kyr. *Geochem. Geophys. Geosyst.* 1919 (55), 1674–1689. doi:10.1029/2017GC007321

Limmer, D. R., Köhler, C. M., Hillier, S., Moreton, S. G., Tabrez, A. R., and Clift, P. D. (2012). Chemical weathering and provenance evolution of Holocene-Recent sediments from the Western Indus Shelf, Northern Arabian Sea inferred from physical and mineralogical properties. *Mar. Geol.* 326-328, 101–115. doi:10.1016/j.margeo.2012.07.009

Lindhorst, S., Betzler, C., and Kroon, D. (2019). Wind variability over the northern Indian Ocean during the past 4 million years – insights from coarse aeolian dust (IODP Exp. 359, Site U1467, Maldives). *Palaeogeogr. Palaeoclimatol. Palaeoecol.* 536, 109371. doi:10.1016/j.palaeo.2019.109371

Lisiecki, L. E., and Raymo, M. E. (2005). A Pliocene-Pleistocene stack of 57 globally distributed benthic $\delta^{18}O$ records. *Paleoceanography* 20, PA1003. doi:10.1029/2004PA001071

Liu, C., Nie, J., Li, Z., Qiao, Q., Abell, J. T., Wang, F., et al. (2021). Eccentricity forcing of East Asian monsoonal systems over the past 3 million years. *Proc. Natl. Acad. Sci. U. S. A.* 118 (43), e2107055118. doi:10.1073/PNAS.2107055118

Liu, Q. S., Deng, C. L., Torrent, J., and Zhu, R. X. (2007). Review of recent developments in mineral magnetism of the Chinese loess. *Quat. Sci. Rev.* 26, 368–385. doi:10.1016/j.quascirev.2006.08.004

Liu, Q. S., Roberts, A. P., Larrasoaña, J. C., Banerjee, S. K., Guyodo, Y., Tauxe, L., et al. (2012). Environmental magnetism: Principles and applications. *Rev. Geophys.* 50 (4), RG4002. doi:10.1029/2012RG000393

Liu, Z., Liu, Q., Torrent, J., Barrón, V., and Hu, P. (2013). Testing the magnetic proxy χ_{FD}/HIRM for quantifying paleoprecipitation in modern soil profilesfrom Shaanxi Province, China. *Glob. Planet. Change* 110, 368–378. doi:10.1016/j.gloplacha.2013.04.013

Liu, Z., Wen, X., Brady, E. C., Otto-Bliesner, B., Yu, G., Lu, H. Y., et al. (2014). Chinese cave records and the East Asia summer monsoon. *Quat. Sci. Rev.* 83, 115–128. doi:10.1016/j.quascirev.2013.10.021

Loulergue, L., Schilt, A., Spahni, R., Masson-Delmotte, V., Blunier, T., Lemieux, B., et al. (2008). Orbital and millennial-scale features of atmospheric CH_4 over the past 800, 000 years. *Nature* 453, 383–386. doi:10.1038/nature06950

Lourens, L. J. (2004). Revised tuning of Ocean Drilling Program Site 964 and KC01B (Mediterranean) and implications for the $\delta^{18}O$, tephra, calcareous nannofossil, and geomagnetic reversal chronologies of the past 1.1 Myr. *Paleoceanography* 19, PA3010. doi:10.1029/2003PA000997

Lu, H., Liu, R., Cheng, L., Feng, H., Zhang, H., Wang, Y., et al. (2020). Phased evolution and variation of the South Asian monsoon, and resulting weathering and surface erosion in the Himalaya–Karakoram Mountains, since late Pliocene time using data from Arabian Sea core. *Geol. Mag.* 157 (6), 864–878. doi:10.1017/S0016756820000291

Lüdmann, T., Kalvelage, C., Betzler, C., Fürstenau, J., and Hübscher, C. (2013). The Maldives, a giant isolated carbonate platform dominated by bottom currents. *Mar. Pet. Geol.* 43, 326–340. doi:10.1016/j.marpetgeo.2013.01.004

Maxbauer, D. P., Feinberg, J. M., Fox, D. L., and Clyde, W. C. (2016). Magnetic minerals as recorders of weathering, diagenesis, and paleoclimate: A core–outcrop comparison of paleocene–eocene paleosols in the bighorn basin, WY, USA. *Earth Planet. Sci. Lett.* 452, 15–26. doi:10.1016/j.epsl.2016.07.029

Michel, F. M., Barron, V., Torrent, J., Morales, M. P., Serna, C. J., Boily, J-F., et al. (2010). Ordered ferrimagnetic form of ferrihydrite reveals links among structure, composition, and magnetism. *Proc. Natl. Acad. Sci. U. S. A.* 107 (7), 2787–2792. doi:10.1073/pnas.0910170107

Milankovitch, M. (1969). *Canon of insolation and the ice-age problem*. Jerusalem: Royal Serbian Academy, Special Publication 1941. No. 132. German by Israel Program for Scientific Translations, translated.

Miriyala, P., Sukumaran, N. P., Nath, B. N., Ramamurty, P. B., Sijinkumar, A. V., Vijayagopal, B., et al. (2017). Increased chemical weathering during the deglacial to mid-Holocene summer monsoon intensification. *Sci. Rep.* 7, 44310. doi:10.1038/srep44310

Mishra, P. K., Anoop, A., Schettler, G., Prasad, S., Jehangir, A., Menzel, P., et al. (2015a). Reconstructed late quaternary hydrological changes from lake tso moriri, NW Himalaya. *Quat. Int.* 371, 76–86. doi:10.1016/j.quaint.2014.11.040

Mishra, P. K., Prasad, S., Anoop, A., Plessen, B., Jehangir, A., Gaye, B., et al. (2015b). Carbonate isotopes from high altitude Tso Moriri Lake (NW Himalayas) provide clues to late glacial and Holocene moisture source and atmospheric circulation changes. *Palaeogeogr. Palaeoclimatol. Palaeoecol.* 425, 76–83. doi:10.1016/j.palaeo.2015.02.031

Mishra, P. K., Prasad, S., Marwan, N., Anoop, A., Krishnan, R., Gaye, B., et al. (2018). Contrasting pattern of hydrological changes during the past two millennia from central and northern India: Regional climate difference or anthropogenic impact? *Glob. Planet. Change* 161, 97–107. doi:10.1016/j.gloplacha.2017.12.005

Misra, P., Tandon, S. K., and aand Sinha, R. (2019). Holocene climate records from lake sediments in India: Assessment of coherence across climate zones. *Earth. Sci. Rev.* 190, 370–397. doi:10.1016/j.earscirev.2018.12.017

Morrill, C., Overpeck, J. T., and Cole, J. E. (2003). A synthesis of abrupt changes in the Asian summer monsoon since the last deglaciation. *Holocene* 13, 465–476. doi:10.1191/0959683603hl639ft

Murray, D. W., and Prell, W. L. (1991). Pliocene to Pleistocene variations in calcium carbonate, organic carbon, and opal on the owen ridge, northern Arabian Sea. *Ocean. Drill. Program Sci. Results* 117, 343–364. doi:10.2973/odp.proc.sr.117.141.1991

Nie, J., Garzione, C., Su, Q., Liu, Q., Zhang, R., Heslop, D., et al. (2017). Dominant 100, 000-year precipitation cyclicity in a late Miocene lake from northeast Tibet. *Sci. Adv.* 3 (3), e1600762. doi:10.1126/sciadv.1600762

Orgeira, M., Egli, R., and Compagnucci, R. (2011). "A quantitative model of magnetic enhancement in loessic soils," in *The Earth's magnetic interior*. Editors E. Petrovský, D. Ivers, T. Harinarayana, and E. Herrero-Bervera (Netherlands: Springer), 361–393. doi:10.1007/978-94-007-0323-0_25

Pandarinath, K. (2009). Clay minerals in SW Indian continental shelf sediment cores as indicators of provenance and palaeomonsoonal conditions: A statistical approach. *Int. Geol. Rev.* 51, 145–165. doi:10.1080/00206810802622112

Pandey, D., Clift, P. D., Kulhanek, D. K., Andò, S., Bendle, J. A. P., Bratenkov, S., et al. (2016). "Site U1456[C]//Arabian Sea monsoon," in *Proceedings of the international ocean discovery program* (College Station, TX: International Ocean Discovery Program), 355. doi:10.14379/iodp.proc.355.102.2016

Paul, A., Reijmer, J., Lampart, J., Kinkel, H., and Betzler, C. (2012). Relationship between Late Pleistocene sea-level variations, carbonate platform morphology and aragonite production (Maldives, Indian Ocean). *Sedimentology* 59, 1640–1658. doi:10.1111/j.1365-3091.2011.01319.x

Pausata, F. S. R., Battisti, D. S., Nisancioglu, K. H., and Bitz, C. M. (2011). Chinese stalagmite $\delta^{18}O$ controlled by changes in the Indian monsoon during a simulated Heinrich event. *Nat. Geosci.* 4, 474–480. doi:10.1038/ngeo1169

Phartiyal, B., Appel, E., Blaha, U., Hoffmann, V., and Kotlia, B. S. (2003). Palaeoclimatic significance of magnetic properties from late quaternary lacustrine sediments at Pithoragarh, Kumaun lesser Himalaya, India. *Quat. Int.* 108, 51–62. doi:10.1016/s1040-6182(02)00193-3

Phartiyal, B., Singh, R., Joshi, P., and Nag, D. (2020). Late-Holocene climatic record from a glacial lake in Ladakh range, Trans-Himalaya, India. *Holocene* 30, 1029–1042. doi:10.1177/0959683620908660

Poulton, S. W., Krom, M. D., and Raiswell, R. (2004). A revised scheme for the reactivity of iron (oxyhydr)oxide minerals towards dissolved sulfide. *Geochim. Cosmochim. Acta* 68, 3703–3715. doi:10.1016/j.gca.2004.03.012

Prasad, S., Anoop, A., Riedel, N., Sarkar, S., Menzel, P., Basavaiah, N., et al. (2014). Prolonged monsoon droughts and links to indo-pacific warm pool: A Holocene record from lonar lake, central India. *Earth Planet. Sci. Lett.* 391, 171–182. doi:10.1016/j.epsl.2014.01.043

Prasad, S., Marwan, N., Eroglu, D., Goswami, B., Mishra, P. K., Gaye, B., et al. (2020). Holocene climate forcings and lacustrine regime shifts in the Indian summer monsoon realm. *Earth Surf. Process. Landf.* 45, 3842–3853. doi:10.1002/esp.5004

Prell, W. L., Berger, A. L., Imbrie, J., Hays, J., and Riedel, D. (1984). "Monsoonal climate of the Arabian Sea during the late quaternary: A response to changing solar radiation," in *Milankovitch and climate, eedited by* (Hingham, 349–366.

Prell, W. L., and Kutzbach, J. E. (1992). Sensitivity of the Indian monsoon to forcing parameters and implications for its evolution. *Nature* 360, 647–652. doi:10.1038/360647a0

Prell, W. L., and Van Campo, E. (1986). Coherent response of Arabian Sea upwelling and pollen transport to late Quaternary monsoonal winds. *Nature* 323, 526–528. doi:10.1038/323526a0

Rasmussen, S. O., Andersen, K. K., Svensson, A., Steffensen, J. P., Vinther, B. M., Clausen, H. B., et al. (2006). A new Greenland ice core chronology for the last glacial termination. *J. Geophys. Res.* 111 (D6), D06102. doi:10.1029/2005JD006079

Rawat, S., Gupta, A. K., Sangode, S. J., Srivastava, P., and Nainwal, H. C. (2015a). Late pleistocene–holocene vegetation and Indian summer monsoon record from the lahaul, northwest Himalaya, India. *Quat. Sci. Rev.* 114, 167–181. doi:10.1016/j.quascirev.2015.01.032

Rawat, S., Gupta, A. K., Srivastava, P., Sangode, S. J., and Nainwal, H. C. (2015b). A 13, 000 year record of environmental magnetic variations in the lake and peat deposits from the Chandra valley, Lahaul: Implications to Holocene monsoonal variability in the NW Himalaya. *Palaeogeogr. Palaeoclimatol. Palaeoecol.* 440, 116–127. doi:10.1016/j.palaeo.2015.08.044

Rawat, S., Phadtare, N. R., and Sangode, S. J. (2012). The Younger Dryas cold event in NW Himalaya based on pollen record from the lake sediments in Himachal Pradesh, India. *Curr. Sci. India* 102, 1193–1198.

Rawat, V., Rawat, S., Srivastava, P., Negi, P. S., Prakasam, M., and Kotlia, B. S. (2021). Middle Holocene Indian summer monsoon variability and its impact on cultural changes in the Indian subcontinent. *Quat. Sci. Rev.* 255, 106825. doi:10.1016/j.quascirev.2021.106825

Rea, D. K. (1992). Delivery of Himalayan sediment to the northern Indian Ocean and its relation to global climate, sea level, uplift, and seawater strontium. *Wash. D.C. Am. Geophys. Union Geophys. Monogr. Ser.* 70, 387–402. doi:10.1029/GM070p0387

Reichart, G.-J., Lourens, L., and Zachariasse, W. (1998). Temporal variability in the northern Arabian Sea oxygen minimum zone (OMZ) during the last 225, 000 years. *Paleoceanography* 13 (6), 607–621. doi:10.1029/98PA02203

Reichart, G. J., den Dulk, M., Visser, H. J., van der Weijden, C. H., and Zachariasse, W. J. (1997). A 22.5 kyr record of dust supply, paleoproductivity and the oxygen minimum zone from the Murray Ridge (northern Arabian Sea). *Palaeogeogr. Palaeoclimatol. Palaeoecol.* 134, 149–169. doi:10.1016/s0031-0182(97)00071-0

Revel, M., Ducassou, E., Grousset, F., Bernasconi, S., Migeon, S., Révillon, S., et al. (2010). 100, 000 years of African monsoon variability recorded in sediments of the Nile margin. *Quat. Sci. Rev.* 29 (11-12), 1342–1362. doi:10.1016/j.quascirev.2010.02.006

Roberts, A. P. (2015). Magnetic mineral diagenesis. *Earth. Sci. Rev.* 151, 1–47. doi:10.1016/j.earscirev.2015.09.010

Rossignol-Strick, M. (1983). African monsoons, an immediate climate response to orbital insolation. *Nature* 304, 46–49. doi:10.1038/304046a0

Ruddiman, W. F. (2001). *Earth's climate: Past and future.* Macmillan.

Ruddiman, W. F. (2006). What is the timing of orbital-scale monsoon changes? *Quat. Sci. Rev.* 25 (7), 657–658. doi:10.1016/j.quascirev.2006.02.004

Saraswat, R., Kurtarkar, S. R., Yadav, R., Mackensen, A., Singh, D. P., Bhadra, S., et al. (2019). Inconsistent change in surface hydrography of the eastern Arabian Sea during the last four glacial-interglacial intervals. *Geol. Mag.* 157 (6), 989–1000. doi:10.1017/S0016756819001122

Schulz, H., von Rad, U., Erlenkeuser, H., and von Rad, U. (1998). Correlation between Arabian Sea and Greenland climate oscillations of the past 110, 000 years. *Nature* 393, 54–57. doi:10.1038/31750

Schwertmann, U. (1993). “Relations between iron oxides, soil color, and soil formation,” in *Soil color*. Editors J. M. Bigham and E. J. Ciolkosz (Madison: Soil Sci. Soc. Am. Spec. Publ.). No. 31.

Sebastian, T., Nath, B. N., Venkateshwarlu, M., Miriyala, P., Prakash, A., Linsy, P., et al. (2019). Impact of the Indian Summer Monsoon variability on the source area weathering in the Indo-Burman ranges during the last 21 ka–A sediment record from the Andaman Sea. *Palaeogeogr. Palaeoclimatol. Palaeoecol.* 516, 22–34. doi:10.1016/j.palaeo.2018.11.035

Shimmield, G. B., Mowbray, R., and Weedon, P. (1990). A 350 ka history of the Indian southwest monsoon—Evidence from deep-sea cores, northwest Arabian Sea. *Trans. R. Soc. Edinb. Earth Sci.* 81, 289–299. doi:10.1017/S0263593300020800

Sinha, A., Cannariato, K. G., Stott, L. D., Li, H.-C., You, C.-F., Cheng, H., et al. (2005). Variability of Southwest Indian summer monsoon precipitation during the Bølling-Allerød. *Geol.* 33 (10), 813–816. doi:10.1130/G21498.1

Sinha, A., Kathayat, G., Cheng, H., Breitenbach, S. F. M., Berkelhammer, M., Mudelsee, M., et al. (2015). Trends and oscillations in the Indian summer monsoon rainfall over the last two millennia. *Nat. Commun.* 6, 6309. doi:10.1038/ncomms7309

Sirocko, F., Garbe-Schonberg, D., and Devey, C. (2000). Processes controlling trace element geochemistry of Arabian Sea sediments during the last 25, 000 years. *Glob. Planet. Change* 26, 217–303. doi:10.1016/S0921-8181(00)00046-1

Snowball, I., Zillén, L., and Sandgren, P. (2002). Bacterial magnetite in Swedish varved lake-sediments: A potential bio-marker of environmental change. *Quat. Int.* 88, 13–19. doi:10.1016/S1040-6182(01)00069-6

Stephanie, S., Silvia, S., Eva, D., Anne-Sophie, B., Colin, C., Erica, L., et al. (2022). Long-term, high-resolution foraminiferal geochemical records ($\delta1^8$O, $\delta1^3$C) from IODP Site 359-U1467. doi:10.1594/PANGAEA.939911

Tabor, C. R., Otto-Bliesner, B. L., Brady, E. C., Nusbaumer, J., Zhu, J., Erb, M. P., et al. (2018). Interpreting precession-driven δ^{18}O variability in the South Asian monsoon region. *J. Geophys. Res. Atmos.* 123, 5927–5946. doi:10.1029/2018JD028424

Tada, R., Zheng, H., and Clift, P. D. (2016). Evolution and variability of the Asian monsoon and its potential linkage with uplift of the Himalaya and Tibetan Plateau. *Prog. Earth Planet. Sci.* 3, 4. doi:10.1186/s40645-016-0080-y

Thamban, M., Rao, V. P., and Schneider, R. R. (2002). Reconstruction of late Quaternary monsoon oscillations based on clay mineral proxies using sediment cores from the Western margin of India. *Mar. Geol.* 186 (3-4), 527–539. doi:10.1016/S0025-3227(02)00268-2

Thamdrup, B. (2000). Bacterial manganese and iron reduction in aquatic sediments. *Adv. Microb. Ecol.* 16, 41–84. doi:10.1007/978-1-4615-4187-5_2

Thompson, R., and Oldfield, F. (1986). *Environmental magnetism*. London: Allen & Unwin.

Tomczak, M., and Godfrey, J. S. (2003). *Regional Oceanography. An introduction*. Delhi: Daya Books.

Torii, M. (1997). Low-temperature oxidation and subsequent downcore dissolution of magnetite in deep-sea sediments, ODP Leg 161 (Western Mediterranean). *J. Geomagn. Geoelec.* 49, 1233–1245. doi:10.5636/jgg.49.1233

Van Campo, E., Duplessy, J.-C., and Rossignol-Strick, M. (1982). Climatic conditions deduced from a 150-kyr oxygen isotope-pollen record from the Arabian Sea. *Nature* 296, 56–59. doi:10.1038/296056a0

Wang, P., Clemens, S., Beaufort, L., Braconnot, P., Ganssen, G., Jian, Z., et al. (2005). Evolution and variability of the asian monsoon system: State of the art and outstanding issues. *Quat. Sci. Rev.* 24 (5), 595–629. doi:10.1016/j.quascirev.2004.10.002

Wang, P. (2009). Global monsoon in a geological perspective. *Sci. Bull.* 54 (7), 1113–1136. (In Chinese with English abstract). CNKI:SUN:KXTB.0.2009-05-003. doi:10.1007/s11434-009-0169-4

Wang, P., Tian, J., Wang, E. Q., and Ma, W. T. (2018). *Earth system and evolution*. Beijing: Science Press.

Wang, P., and Wang, Z. B. (2006). [Suggestions on amendments of appendix of "occupational health monitoring control measures"]. *Quat. Sci.* 26 (5), 694–701. (In Chinese with English abstract). doi:10.3321/j.issn:1001-7410.2006.05.003

Wang, P. X., Wang, B., Cheng, H., Fasullo, J., Guo, Z., Kiefer, T., et al. (2014). The global monsoon across time scales: Coherent variability of regional monsoons. *Clim. Past.* 10, 2007–2052. doi:10.5194/cp-10-2007-2014

Wang, P. X., Wang, B., Cheng, H., Fasullo, J., Guo, Z. T., Kiefer, T., et al. (2017). The global monsoon across time scales: Mechanisms and outstanding issues. *Earth. Sci. Rev.* 174, 84–121. doi:10.1016/j.earscirev.2017.07.006

Wang, Y. J., Cheng, H., Edwards, R. L., An, Z. S., Wu, J. Y., Shen, C.-C., et al. (2001). A high-resolution absolute-dated Late Pleistocene monsoon record from Hulu cave, China. *Science* 294 (5550), 2345–2348. doi:10.1126/science.1064618

Wang, Y. J., Cheng, H., Edwards, R. L., Kong, X., Shao, X., Chen, S., et al. (2008). Millennial- and orbital-scale changes in the East Asian monsoon over the past 224, 000 years. *Nature* 451, 1090–1093. doi:10.1038/nature06692

Wang, Y., Shen, J., Wang, Y., Liu, X., Cao, X., and Herzschuh, U. (2020). Abrupt mid-Holocene decline in the Indian Summer Monsoon caused by tropical Indian Ocean cooling. *Clim. Dyn.* 55, 1961–1977. doi:10.1007/s00382-020-05363-7

Weber, M. E., Lantzsch, H., Dekens, P., Das, S. K., Reilly, B. T., Martos, Y. M., et al. (2018). 200, 000 years of monsoonal history recorded on the lower Bengal Fan-strong response to insolation forcing. *Glob. Planet. Change* 166, 107–119. doi:10.1016/j.gloplacha.2018.04.003

Weber, M. E., Wiedick-Hombach, M., Kudrass, H. R., and Erlenkeuser, H. (2003). Bengal Fan sediment transport activity and response to climate forcing inferred from sediment physical properties. *Sediment. Geol.* 155 (3), 361–381. doi:10.1016/S0037-0738(02)00187-2

Webster, P. J., Magana, V. O., Palmer, T., Shukla, J., Tomas, R., Yanai, M., et al. (1998). Monsoons: Processes, predictability, and the prospects for prediction. *J. Geophys. Res.* 103 (C7), 14451–14510. doi:10.1029/97JC02719

Xu, X. W., Qiang, X. K., Li, X. B., Qiu, H. J., Zhao, H., Fu, C. F., et al. (2022). Determination of the optimized late Pleistocene chronology of a lacustrine sedimentary core from the Heqing Basin by geomagnetic paleointensity and its paleoclimate significance. *Catena* 212, 106095. doi:10.1016/J.CATENA.2022.106095

Yang, X., Peng, X., Qiang, X., Li, N., Zhou, Q., and Wang, Y. (2016). Chemical weathering intensity and terrigenous flux in south China during the last 90, 000 years-evidence from magnetic signals in marine sediments. *Front. Earth Sci.* 4 (47). doi:10.3389/feart.2016.00047

Yin, Q. Z., and Guo, Z. T. (2007). Strong summer monsoon during the cool MIS-13. *Clim. Past.* 3 (5), 29–34. doi:10.5194/cp-4-29-2008

Yuan, D., Cheng, H., Edwards, R. L., Dykoski, C. A., Kelly, M. J., Zhang, M., et al. (2004). Timing, duration, and transitions of the last interglacial Asian monsoon. *Science* 304 (5670), 575–578. doi:10.1126/science.1091220

Zhang, Q., Liu, Q., and Sun, Y. (2019). Review of recent developments in aeolian dust signals of sediments from the North Pacific Ocean based on magnetic minerals. *Geol. Mag.* 157 (5), 790–805. doi:10.1017/S0016756819000712

Ziegler, M., Lourens, L. J., Tuenter, E., Hilgen, F., Reichart, G. J., and Weber, N. (2010a). Precession phasing offset between Indian summer monsoon and Arabian Sea productivity linked to changes in Atlantic overturning circulation. *Paleoceanography* 25, PA3213. doi:10.1029/2009PA001884

Ziegler, M., Lourens, L. J., Tuenter, E., and Reichart, G.-J. (2010b). High Arabian Sea productivity conditions during MIS 13-odd monsoon event or intensified overturning circulation at the end of the Mid-Pleistocene transition? *Clim. Past.* 6 (1), 63–76. doi:10.5194/cp-6-63-2010